Euro. Jnl of Applied Mathematics (2007), *vol.* 18, *pp.* 709–743.
doi:10.1017/S0956792507007188 Printed in the United Kingdom

A Survey in Mathematics for Industry
Multirate partial differential algebraic equations for simulating radio frequency signals

ROLAND PULCH, MICHAEL GÜNTHER and STEPHANIE KNORR

Lehrstuhl für Angewandte Mathematik und Numerische Analysis,
Bergische Universität Wuppertal, Gaußstr. 20, D-42119 Wuppertal, Germany
E-mail: [pulch,guenther,knorr]@math.uni-wuppertal.de

(*Received 19 September 2006; revised 27 July 2007; first published online 16 November 2007*)

In radio frequency (RF) applications, electric circuits produce signals exhibiting fast oscillations, whereas the amplitude and frequency may change slowly in time. Thus, solving a system of differential algebraic equations (DAEs), which describes the circuit's transient behaviour, becomes inefficient, since the fast rate restricts the step sizes in time. A multivariate model is able to decouple the widely separated time scales of RF signals and provides an alternative approach. Consequently, a system of DAEs changes into a system of multirate partial differential algebraic equations (MPDAEs). The determination of multivariate solutions allows for the exact reconstruction of corresponding time-dependent signals. Hence, an efficient numerical simulation is obtained by exploiting the periodicities in fast time scales. We outline the theory of this multivariate approach with respect to the simulation of amplitude as well as frequency modulated signals. Furthermore, a survey of numerical methods for solving the arising problems of MPDAEs is given.

1 Introduction

In many applications, technical systems comprise parts that evolve at largely differing time scales: for example, in vehicle system dynamics, the interaction of catenary and pantograph links the fast mode of the catenary with the relatively slow dynamics of the vehicle [34]; in chip design, often only small subsystems of a chip are active, whereas the largest part is evolving quite slowly or remains nearly inactive [35]. To exploit this multiscale behaviour in time, specialised schemes have been and are currently developed, which do not use a joint step size defined by the fastest mode for the whole system, but employ this multirate potential by treating each subsystem with an appropriate time stepping, see [8] for an overview.

Another source of multiscale behaviour are multitone systems. Here, the multirate behaviour cannot be localised at subsystem level, but is spread over the whole system: each function of the solution itself combines a dynamical behaviour at different, usually widely separated time scales. This type of multirate behaviour is typical for radio frequency (RF) circuits, which are in the core of today's telecommunication systems.

In an industrial framework, electrical networks in general and RF circuits in particular are usually modelled by applying the modified nodal approach (MNA) [12]. Written in a

compact way, this approach results in the MNA network equations

$$\frac{\mathrm{d}}{\mathrm{d}t}\,\mathbf{q}(\mathbf{x}(t)) = \mathbf{f}(\mathbf{b}(t), \mathbf{x}(t)), \tag{1.1}$$

where the unknown voltages and currents are collected in $\mathbf{x} : \mathbb{R} \to \mathbb{R}^k$. The functions $\mathbf{q} : \mathbb{R}^k \to \mathbb{R}^k$ comprise charges and fluxes, and the right-hand side $\mathbf{f} : \mathbb{R}^s \times \mathbb{R}^k \to \mathbb{R}^k$ contains time-dependent input signals $\mathbf{b} : \mathbb{R} \to \mathbb{R}^s$. As the Jacobian $\partial\mathbf{q}(\mathbf{x})/\partial\mathbf{x}$ is singular in general, one has to deal with differential algebraic equations (DAEs).

This paper aims at giving a survey on how to model and simulate numerically these systems in an appropriate, i.e., fast, robust and reliable way if the involved signals exhibit a multitone behaviour. Accordingly, a multivariate model can be employed to represent the signals. Hence, the differential algebraic system (1.1) is analytically transformed into a singular system of partial differential equations, the so-called multirate partial differential algebraic equations (MPDAEs). The MPDAE system can be solved more efficiently than the original DAE description, since time scales are decoupled.

Alternatively, Gautschi type methods and approaches based on Magnus series (see [9]) have been designed for highly oscillatory systems (1.1). These techniques solve initial value problems efficiently if the system exhibits a weakly non-linear structure. In contrast, the MPDAE approach allows for simulating strongly non-linear systems. Moreover, boundary conditions can be directly imposed in the multivariate domain of dependence.

The paper is organised as follows. In Section 2, we deal with systems that feature a pure amplitude modulation (AM) and, thus, exhibit constant time rates. We start with a careful discussion of the MPDAE approach based on a multivariate model for amplitude modulated signals and use the specific structure of the MPDAE system to verify the well-posedness of the system. Section 3 is devoted to systems with frequency modulation (FM), which do not possess constant time rates. On the basis of a multivariate model for frequency modulated signals, we consider a warped MPDAE model as generalisation of the approach for amplitude modulated signals. The so-called local frequency function will turn out to be some kind of a generalised modelling parameter, which enables different but analytically equivalent descriptions of the RF circuits, provided that some transformation properties are satisfied. Conditions for an appropriate choice of this modelling parameter can be based on simple boundary conditions or on solving optimisation problems. In each chapter, a second part gives an overview on numerical methods proposed so far in the literature, which can be classified as frequency, time or mixed domain methods. Both sections are completed by a careful discussion of an illustrative example, the ring modulator and the Colpitt oscillator, respectively. Finally, in Section 4, we formulate important open questions, which need to be addressed in the future.

2 Model for constant frequencies

In this section, we consider the case of multitone signals in RF circuits, in which the occurring time rates are forced by independent inputs and, thus, are constant. Consequently, the multidimensional model employs constant frequencies for the representation as well as the numerical simulation of such signals.

https://doi.org/10.1017/S0956792507007188 Published online by Cambridge University Press

2.1 Multidimensional approach

2.1.1 *Multivariate model for AM signals*

The idea to cope with widely separated time scales is to introduce a corresponding variable to each of them. The multidimensional representation of a signal is then called *multivariate function (MVF)*. A quasiperiodic signal $\mathbf{x} : \mathbb{R} \to \mathbb{C}^k$ with m fundamental frequencies $\omega_l = 2\pi/T_l$, $l = 1, \ldots, m$, can be represented via

$$\mathbf{x}(t) = \sum_{j_1=-\infty}^{\infty} \cdots \sum_{j_m=-\infty}^{\infty} \mathbf{X}_{j_1,\ldots,j_m} \exp(i(j_1\omega_1 + \cdots + j_m\omega_m)\, t), \tag{2.1}$$

where $\mathbf{X}_{j_1,\ldots,j_m} \in \mathbb{C}^k$ and $i = \sqrt{-1}$. This multirate structure leads naturally to the corresponding MVF $\hat{\mathbf{x}} : \mathbb{R}^m \to \mathbb{C}^k$ with

$$\hat{\mathbf{x}}(t_1, \ldots, t_m) = \sum_{j_1=-\infty}^{\infty} \cdots \sum_{j_m=-\infty}^{\infty} \mathbf{X}_{j_1,\ldots,j_m} \exp(i(j_1\omega_1 t_1 + \cdots + j_m\omega_m t_m)). \tag{2.2}$$

Now, the time scales are decoupled in the multidimensional model. Moreover, the MVF is periodic in each coordinate direction. The original signal is contained in the MVF and can be reconstructed by $\mathbf{x}(t) = \hat{\mathbf{x}}(t, \ldots, t)$, which follows the diagonal direction. This procedure is also applicable if the fundamental frequencies $\omega_1, \ldots, \omega_m$ are commensurable.

For illustration, we introduce a two-tone quasiperiodic signal $x : \mathbb{R} \to \mathbb{R}$,

$$x(t) := \left[1 + \alpha \sin\left(\frac{2\pi}{T_1} t\right)\right] \cdot \sin\left(\frac{2\pi}{T_2} t\right) \tag{2.3}$$

with $0 < \alpha < 1$, which exhibits amplitude modulation including two different time scales $T_1 > T_2$. Its MVF $\hat{x} : \mathbb{R}^2 \to \mathbb{R}$ is derived as follows:

$$\hat{x}(t_1, t_2) = \left[1 + \alpha \sin\left(\frac{2\pi}{T_1} t_1\right)\right] \cdot \sin\left(\frac{2\pi}{T_2} t_2\right). \tag{2.4}$$

Figure 1 shows the signal and its MVF, which is defined in the rectangle $[0, T_1] \times [0, T_2]$. The more the time scales differ ($T_1 \gg T_2$), the more efficient the multidimensional approach becomes, since the structure of the MVF is independent of the ratio T_1/T_2.

In the case of m different time scales with $m - 1$ periodic and one aperiodic scale, we consider envelope-modulated signals

$$\mathbf{x}(t) = \sum_{j_2=-\infty}^{\infty} \cdots \sum_{j_m=-\infty}^{\infty} \mathbf{X}_{j_2,\ldots,j_m}(t) \exp(i(j_2\omega_2 + \cdots + j_m\omega_m)\, t) \tag{2.5}$$

with functions $\mathbf{X}_{j_2,\ldots,j_m} : \mathbb{R} \to \mathbb{C}^k$. Usually, the aperiodic part is the slowest time scale. The MVF is obtained analogously to the quasiperiodic case with $\mathbf{X}_{j_2,\ldots,j_m}$ then depending on t_1. Hence, signals of this type can also be represented efficiently by the multidimensional approach.

https://doi.org/10.1017/S0956792507007188 Published online by Cambridge University Press

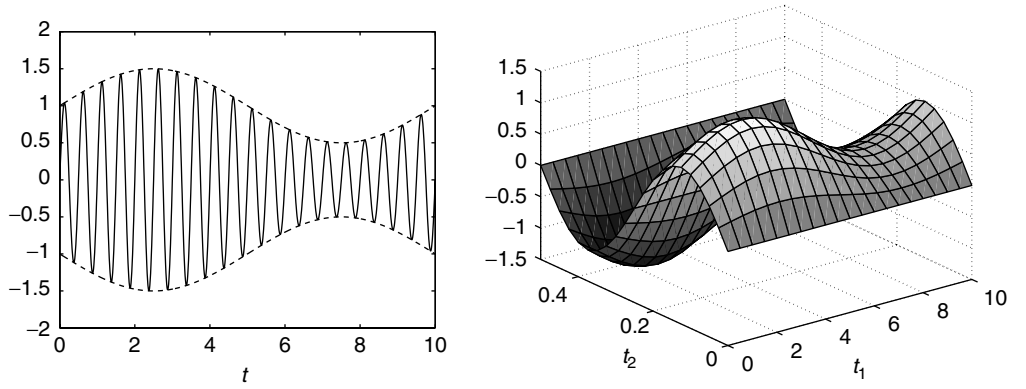

FIGURE 1. Signal x (left) and its multivariate function $\hat{x}$ (right).

2.1.2 *MPDAE model*

Now, we apply the multidimensional signal model to solutions of the differential algebraic network equations (1.1), which have been established in Section 1. To determine quasiperiodic solutions (2.1) on the level of the DAEs (1.1), time and frequency domain methods have been introduced in [5] and [37], respectively.

Assuming m different time scales, we introduce MVFs $\hat{\mathbf{x}} : \mathbb{R}^m \to \mathbb{R}^k$ of the unknowns and $\hat{\mathbf{b}} : \mathbb{R}^m \to \mathbb{R}^s$ of the input signals. Considering the DAEs (1.1), Brachtendorf *et al.* [2] introduce the corresponding *multirate partial differential algebraic equations* (*MPDAEs*),

$$\frac{\partial \mathbf{q}(\hat{\mathbf{x}})}{\partial t_1} + \cdots + \frac{\partial \mathbf{q}(\hat{\mathbf{x}})}{\partial t_m} = \mathbf{f}(\hat{\mathbf{b}}(t_1, \ldots, t_m), \hat{\mathbf{x}}(t_1, \ldots, t_m)). \tag{2.6}$$

Given a solution of the MPDAE (2.6), we can reconstruct a solution of the original DAE (1.1) by

$$\mathbf{x}(t) = \hat{\mathbf{x}}(t, \ldots, t), \tag{2.7}$$

see [2]. To solve the MPDAE, we have to impose boundary conditions, which determine the structure of the obtained solution. If the inputs $\mathbf{b}$ of (1.1) are quasiperiodic, then a quasiperiodic output $\mathbf{x}$ with identical time rates is expected. Looking for an m-tone quasiperiodic solution (2.1) of the DAE, we solve the MPDAE for an m-periodic MVF satisfying the boundary conditions

$$\hat{\mathbf{x}}(t_1, \ldots, t_m) = \hat{\mathbf{x}}(t_1 + k_1 T_1, \ldots, t_m + k_m T_m) \quad \begin{array}{l} \text{for all } t_1, \ldots, t_m \in \mathbb{R}, \\ \text{and } k_1, \ldots, k_m \in \mathbb{Z}. \end{array} \tag{2.8}$$

Considering envelope-modulated signals (2.5) with $m-1$ periodic rates and one aperiodic time scale, we solve an initial-boundary value problem

$$\begin{array}{ll} \hat{\mathbf{x}}(0, t_2, \ldots, t_m) = \mathbf{h}(t_2, \ldots, t_m) & \text{for all } t_2, \ldots, t_m \in \mathbb{R}, \\ \hat{\mathbf{x}}(t_1, t_2, \ldots, t_m) = \hat{\mathbf{x}}(t_1, t_2 + k_2 T_2, \ldots, t_m + k_m T_m) & \begin{array}{l} \text{for all } t_1, \ldots, t_m \in \mathbb{R}, \\ \text{and } k_2, \ldots, k_m \in \mathbb{Z}. \end{array} \end{array} \tag{2.9}$$

https://doi.org/10.1017/S0956792507007188 Published online by Cambridge University Press

The function $\mathbf{h}$ has to be prescribed appropriately. It follows that the reconstructed signal (2.7) depends only on $\mathbf{h}(0,\dots,0)$, i.e., for every function $\mathbf{h}$ with $\mathbf{h}(0,\dots,0) = \mathbf{x}(0)$, the same solution will be obtained. For a more detailed description of the relation between DAE and MPDAE solutions, we refer to Roychowdhury [33].

Usually, systems exhibiting exactly two different time scales occur in practice,

$$\frac{\partial \mathbf{q}(\hat{\mathbf{x}})}{\partial t_1} + \frac{\partial \mathbf{q}(\hat{\mathbf{x}})}{\partial t_2} = \mathbf{f}(\hat{\mathbf{b}}(t_1, t_2), \hat{\mathbf{x}}(t_1, t_2)). \tag{2.10}$$

The corresponding biperiodic boundary conditions read

$$\begin{aligned} \hat{\mathbf{x}}(t_1, t_2) &= \hat{\mathbf{x}}(t_1 + T_1, t_2) \quad \text{for all } \ t_1, t_2 \in \mathbb{R}, \\ \hat{\mathbf{x}}(t_1, t_2) &= \hat{\mathbf{x}}(t_1, t_2 + T_2) \quad \text{for all } \ t_1, t_2 \in \mathbb{R}, \end{aligned} \tag{2.11}$$

and the initial-boundary value problem is solved with

$$\begin{aligned} \hat{\mathbf{x}}(0, t_2) &= \mathbf{h}(t_2) \qquad\qquad \text{for all } \ t_2 \in \mathbb{R}, \\ \hat{\mathbf{x}}(t_1, t_2) &= \hat{\mathbf{x}}(t_1, t_2 + T_2) \quad \text{for all } \ t_1, t_2 \in \mathbb{R}. \end{aligned} \tag{2.12}$$

The initial-boundary value problem can also be used to determine biperiodic solutions in case of quasiperiodic input signals. Accordingly, the problem is solved by proceeding in t_1-direction until the solution enters a biperiodic steady state response. This strategy can be seen as a multidimensional generalisation of transient analysis by applying more information about the signal structure. Furthermore, if the input signals are periodic with only one time rate, then the problem (2.12) using two time scales also yields periodic responses of the DAE (1.1). Starting from some initial condition, the MPDAE (2.10) is solved until the solution reaches a periodic signal, i.e., the Fourier coefficients in (2.5) become constant.

Before considering numerical schemes, we investigate the structure of the MPDAE and the well-posedness of the problem.

2.1.3 *Characteristic system of the MPDAE*

The following results are based on the special structure of the MPDAE (2.6) and its inherent partial differential equation (PDE), which have been investigated in [24]. In this paper, we only give a short overview of the basic ideas.

The inherent PDE of system (2.6) is of hyperbolic type, where each component of the system consists of a derivative in direction of the diagonal. Thus, the information transport takes place along *characteristic curves*, which are straight lines in diagonal direction. The algebraic constraints in case of DAEs do not affect this information transport and we are able to formulate the characteristic system of (2.6),

$$\begin{aligned} &\frac{\mathrm{d}}{\mathrm{d}\tau} t_l(\tau) = 1, \quad l = 1, \dots, m, \\ &\frac{\mathrm{d}}{\mathrm{d}\tau} \mathbf{q}(\hat{\mathbf{x}}(\tau)) = \mathbf{f}(\hat{\mathbf{b}}(t_1(\tau), \dots, t_m(\tau)), \hat{\mathbf{x}}(\tau)). \end{aligned} \tag{2.13}$$

Thereby, the time variables as well as the MVF of the solution depend on a parameter τ.

https://doi.org/10.1017/S0956792507007188 Published online by Cambridge University Press

The part corresponding to the time variables can be solved explicitly. Hence, we obtain the *characteristic projections*

$$(t_1(\tau),\dots,t_m(\tau)) = (\tau + c_1,\dots,\tau + c_m) \quad \text{for arbitrary } c_1,\dots,c_m \in \mathbb{R}. \tag{2.14}$$

The characteristic projections represent a continuum of parallel straight lines in the domain of dependence. Inserting this result in the last equation of the characteristic system (2.13) yields

$$\frac{\mathrm{d}}{\mathrm{d}\tau}\mathbf{q}(\hat{\mathbf{x}}(\tau)) = \mathbf{f}(\hat{\mathbf{b}}(\tau + c_1,\dots,\tau + c_m), \hat{\mathbf{x}}(\tau)). \tag{2.15}$$

This family of DAE systems completely describes the transport of information in the system of MPDAEs (2.6).

Due to the hyperbolic structure of the system, Cauchy initial value problems are well-posed provided that initial conditions are consistent. Moreover, the structure can be used to solve multiperiodic boundary value problems numerically, as we will see in Section 2.2.

2.1.4 *Well-posedness of problems*

To investigate the properties of the MPDAE system (2.6) with respect to algebraic constraints, we have to write the original DAE of the network approach in a more detailed manner. Excluding controlled sources, modified nodal analysis [7, 12] leads to the system

$$A_C\dot{\tilde{\mathbf{q}}} + A_R\mathbf{r}\big(A_R^\top\mathbf{u}(t), t\big) + A_L\boldsymbol{\jmath}_L(t) + A_V\boldsymbol{\jmath}_V(t) + A_I\boldsymbol{\imath}(t) = \mathbf{0}, \tag{2.16a}$$

$$\dot{\boldsymbol{\Phi}} - A_L^\top\mathbf{u}(t) = \mathbf{0}, \tag{2.16b}$$

$$A_V^\top\mathbf{u}(t) - \mathbf{v}(t) = \mathbf{0}, \tag{2.16c}$$

$$\tilde{\mathbf{q}} - \mathbf{q}_C\big(A_C^\top\mathbf{u}(t), t\big) = \mathbf{0}, \tag{2.16d}$$

$$\boldsymbol{\Phi} - \boldsymbol{\Phi}_L(\boldsymbol{\jmath}_L(t), t) = \mathbf{0}. \tag{2.16e}$$

The incidence matrices A_C, A_R, A_L and A_V, A_I are associated with capacitive, resistive, inductive parts of the network and with branches including independent voltage and current sources, respectively. Correspondingly, we denote charges by $\tilde{\mathbf{q}}$, fluxes by $\boldsymbol{\Phi}$, resistances by $\mathbf{r}$, current sources by $\boldsymbol{\imath}$ and voltage sources by $\mathbf{v}$. The state variables $(\mathbf{u}, \boldsymbol{\jmath}_L, \boldsymbol{\jmath}_V)^\top$ are node potentials and currents through inductances and voltage sources. To shorten the notation, we will from now on skip the time dependence of the state variables.

In [16], the multidimensional signal model is applied to the system (2.16) and the structural properties of the resulting "detailed version" of an MPDAE are investigated. For this purpose, the MPDAE is split into a semi-explicit system of PDEs and algebraic equations. This is done by means of orthogonal projectors following techniques proposed by Estèvez Schwarz and Tischendorf [6], who carry out the splitting for the original network-DAE (2.16).

As the derivation of the MPDAE's semi-explicit formulation is rather technical and lengthy, we show an equivalent approach, where we start from the semi-explicit

https://doi.org/10.1017/S0956792507007188 Published online by Cambridge University Press

DAE-formulation due to [6] and then introduce the multidimensional signal model. Thereby, we do not have to deal with the various projectors, which are needed to split the equations, but we can focus on the transfer by MVFs.

The relation of index properties of the differential algebraic network equations and topological conditions of the circuit have also been investigated by Tischendorf [36]. The network-DAE (2.16) has differential index 1, if the following two topological conditions are satisfied:

T1: There are no cutsets consisting of inductances and/or current sources only: $\ker(A_C, A_R, A_V)^\top = \{\mathbf{0}\}$.

T2: There are no loops consisting of only capacitances and at least one voltage source: $\ker Q_C^\top A_V = \{\mathbf{0}\}$.

In [6], the authors prove that the system (2.16) can then be written in the semi-explicit form

$$\begin{aligned} P_C\dot{\mathbf{u}} &= -H_1^{-1}\left(A_C^\top\mathbf{u},t\right)P_C^\top\Big[A_C\frac{\partial}{\partial t}\mathbf{q}_C\left(A_C^\top\mathbf{u},t\right) \\ &\quad + A_R\mathbf{r}\left(A_R^\top\mathbf{u},t\right) + A_L\boldsymbol{J}_L + A_V\boldsymbol{J}_V + A_I\boldsymbol{\imath}(t)\Big], \qquad (2.17a) \\ \dot{\boldsymbol{J}}_L &= L^{-1}(\boldsymbol{J}_L,t)\left(A_L^\top\mathbf{u} - \frac{\partial}{\partial t}\boldsymbol{\Phi}_L(\boldsymbol{J}_L,t)\right), \qquad (2.17b) \\ \mathbf{0} &= Q_C^\top\left[A_R\mathbf{r}\left(A_R^\top\mathbf{u},t\right) + A_L\boldsymbol{J}_L + A_V\boldsymbol{J}_V + A_I\boldsymbol{\imath}(t)\right], \qquad (2.17c) \\ \mathbf{0} &= A_V^\top\mathbf{u} - \mathbf{v}(t). \qquad (2.17d) \end{aligned}$$

This is done using the orthogonal projectors Q_C onto the kernel of $A_C^\top$, and P_C such that $Q_C + P_C = I$. The capacitance and inductance matrices

$$C(\mathbf{w},t) := \frac{\partial\mathbf{q}_C(\mathbf{w},t)}{\partial\mathbf{w}} \quad \text{and} \quad L(\mathbf{w},t) := \frac{\partial\boldsymbol{\Phi}_L(\mathbf{w},t)}{\partial\mathbf{w}} \qquad (2.18)$$

as well as the matrix

$$H_1\left(A_C^\top\mathbf{u},t\right) := A_C C\left(A_C^\top\mathbf{u},t\right)A_C^\top + Q_C^\top Q_C \qquad (2.19)$$

are positive definite. Thus, the system (2.17) defines differential equations for $P_C\mathbf{u}$ and $\boldsymbol{J}_L$ and two constraints, which can be resolved for the algebraic variables $Q_C\mathbf{u}$ and $\boldsymbol{J}_V$.

We apply the multidimensional signal model for the biperiodic case of two different time scales and represent each time-dependent function occurring in (2.17) by its MVF. Moreover, we introduce the matrices

$$\hat{C}(\mathbf{w},t_1,t_2) := \frac{\partial\hat{\mathbf{q}}_C(\mathbf{w},t_1,t_2)}{\partial\mathbf{w}} \quad \text{and} \quad \hat{L}(\mathbf{w},t_1,t_2) := \frac{\partial\hat{\boldsymbol{\Phi}}_L(\mathbf{w},t_1,t_2)}{\partial\mathbf{w}}, \qquad (2.20)$$

which are assumed to be positive definite with a globally bounded inverse on the domain $[0,T_1]\times[0,T_2]$ defined by the time scales.

https://doi.org/10.1017/S0956792507007188 Published online by Cambridge University Press

Altogether, we obtain the semi-explicit MPDAE system

$$\begin{aligned}
\frac{\partial P_C\hat{\mathbf{u}}}{\partial t_1}+\frac{\partial P_C\hat{\mathbf{u}}}{\partial t_2} &= -\hat{H}_1^{-1}\big(A_C^\top\hat{\mathbf{u}},t_1,t_2\big)P_C^\top\left[A_C\left(\frac{\partial\hat{\mathbf{q}}_C}{\partial t_1}+\frac{\partial\hat{\mathbf{q}}_C}{\partial t_2}\right)\big(A_C^\top\hat{\mathbf{u}},t_1,t_2\big)\right.\\
&\quad\left.+A_R\hat{\mathbf{r}}\big(A_R^\top\hat{\mathbf{u}},t_1,t_2\big)+A_L\hat{\boldsymbol{\jmath}}_L+A_V\hat{\boldsymbol{\jmath}}_V+A_I\hat{\boldsymbol{\imath}}(t_1,t_2)\right], \qquad (2.21a)\\
\frac{\partial\hat{\boldsymbol{\jmath}}_L}{\partial t_1}+\frac{\partial\hat{\boldsymbol{\jmath}}_L}{\partial t_2} &= \hat{L}^{-1}(\hat{\boldsymbol{\jmath}}_L,t_1,t_2)\left(A_L^\top\hat{\mathbf{u}}-\left(\frac{\partial\hat{\boldsymbol{\Phi}}_L}{\partial t_1}+\frac{\partial\hat{\boldsymbol{\Phi}}_L}{\partial t_2}\right)(\hat{\boldsymbol{\jmath}}_L,t_1,t_2)\right), \qquad (2.21b)\\
\mathbf{0} &= Q_C^\top\left[A_R\hat{\mathbf{r}}\big(A_R^\top\hat{\mathbf{u}},t_1,t_2\big)+A_L\hat{\boldsymbol{\jmath}}_L+A_V\hat{\boldsymbol{\jmath}}_V+A_I\hat{\boldsymbol{\imath}}(t_1,t_2)\right], \qquad (2.21c)\\
\mathbf{0} &= A_V^\top\hat{\mathbf{u}}-\hat{\mathbf{v}}(t_1,t_2), \qquad (2.21d)
\end{aligned}$$

where again the matrix

$$\hat{H}_1\big(A_C^\top\hat{\mathbf{u}},t_1,t_2\big) := A_C\hat{C}\big(A_C^\top\hat{\mathbf{u}},t_1,t_2\big)A_C^\top+Q_C^\top Q_C \qquad (2.22)$$

is positive definite by construction. The two constraints (2.21c) and (2.21d) are resolvable for the algebraic variables $Q_C\hat{\mathbf{u}}$ and $\hat{\boldsymbol{\jmath}}_V$, iff the topological conditions T1 and T2 hold. Thus, similar to the case of DAEs, the MPDAE-formulation of (2.16) is represented by a PDE on a manifold, which can be written as a so-called "underlying PDE" (cf. [16]).

If one of the topological conditions is violated, the network-DAE (2.16) is of index 2. In this case, the system can also be written in a semi-explicit form, where the algebraic variables of (2.17) are split into index 1 and index 2 variables using further orthogonal projectors. Applying the multidimensional signal model again yields a semi-explicit MPDAE, which can also be derived starting from the MPDAE-formulation of (2.16) and then splitting the MVFs of the network variables via the same orthogonal projectors.

In both, index 1 and index 2 cases of the network-DAE, the corresponding MPDAE inherits all the structural properties of the original system. Moreover, when looking at the characteristic system (2.15), we also retrieve the structure of the original network-DAE (2.16). Due to the particular structure, it seems natural to assign index concepts for DAEs to the MPDAE system. Therefore, we do not expect additional stability problems, when solving the network equations via the multidimensional approach.

For the general DAE-formulation (1.1), a comparison to (2.16) yields

$$\mathbf{x} := (\tilde{\mathbf{q}},\boldsymbol{\Phi},\mathbf{u},\boldsymbol{\jmath}_L,\boldsymbol{\jmath}_V)^\top, \quad \mathbf{q}(\mathbf{x}) := (A_C\tilde{\mathbf{q}},\boldsymbol{\Phi},\mathbf{0},\mathbf{0},\mathbf{0})^\top \qquad (2.23)$$

and the remaining terms comprise the right-hand side with the time-dependent input signals. Thus, the network-DAEs (2.16) represent a special case of (1.1), where a linear function $\mathbf{q}$ is present. Furthermore, the general form (1.1) includes a broad class of DAEs obtained by other mathematical models of electric circuits than MNA (see [15] for examples). For simplicity, we use the compact formulation (1.1) to outline numerical methods in the following sections.

https://doi.org/10.1017/S0956792507007188 Published online by Cambridge University Press

2.2 Numerical methods

In this section, we describe numerical methods for solving initial-boundary value problems (2.9) as well as multiperiodic boundary value problems (2.8) of the MPDAE system. Thereby, we restrict out attention to the case of two time scales, since generalisations to three or more time variables are straightforward. Consequently, we consider the MPDAE (2.10) in the following.

2.2.1 *Frequency domain methods*

Brachtendorf *et al.* [2] introduce a method for determining biperiodic solutions according to (2.11) purely in the frequency domain. Therefore, both time scales have to be periodic, since a representation using Fourier coefficients is applied for each variable. This strategy can be regarded as a multidimensional generalisation of the harmonic balance technique.

The approximation is obtained via a Galerkin approach. The MPDAE implies the definition of the residual

$$\mathbf{r}(t_1,t_2) := \frac{\partial \mathbf{q}(\hat{\mathbf{x}})}{\partial t_1}(t_1,t_2) + \frac{\partial \mathbf{q}(\hat{\mathbf{x}})}{\partial t_2}(t_1,t_2) - \mathbf{f}(\hat{\mathbf{b}}(t_1,t_2),\hat{\mathbf{x}}(t_1,t_2)) \tag{2.24}$$

and thus, the corresponding weak formulation reads

$$\frac{1}{T_1 T_2}\int_0^{T_1}\int_0^{T_2} \mathbf{r}(t_1,t_2)\cdot\overline{\boldsymbol{\Psi}(t_1,t_2)}\,\mathrm{d}t_2\,\mathrm{d}t_1 = \mathbf{0} \tag{2.25}$$

for all test functions $\boldsymbol{\Psi} : \mathbb{R}^2 \to \mathbb{C}^k$. Here, the integration, multiplication and complex conjugation operate on each component $l = 1,\ldots,k$, separately. The unknown solution is approximated by a finite sum of two-dimensional trigonometric polynomials

$$\hat{\mathbf{x}}(t_1,t_2) \doteq \sum_{j_1=-p_1}^{p_1}\sum_{j_2=-p_2}^{p_2} \hat{\mathbf{X}}_{j_1,j_2}\exp\left(i(\omega_1 j_1 t_1 + \omega_2 j_2 t_2)\right) \tag{2.26}$$

with $\hat{\mathbf{X}}_{j_1,j_2} \in \mathbb{C}^k$ and frequencies $\omega_l = 2\pi/T_l$ for $l = 1,2$. This approximation is biperiodic due to its construction. The basis functions used in the sum (2.26) form an orthogonal system with respect to the sesquilinear form corresponding to (2.25). Let $\hat{\mathbf{Q}}_{j_1,j_2}$ and $\hat{\mathbf{F}}_{j_1,j_2}$ be the according Fourier coefficients of the biperiodic functions $\mathbf{q}(\hat{\mathbf{x}})$ and $\mathbf{f}(\hat{\mathbf{b}},\hat{\mathbf{x}})$, respectively. These values depend on all unknowns $\hat{\mathbf{X}} := (\hat{\mathbf{X}}_{j_1,j_2})$. Now, the partial derivatives can be evaluated explicitly

$$\begin{aligned}&\frac{\partial \mathbf{q}(\hat{\mathbf{x}})}{\partial t_1}(t_1,t_2) + \frac{\partial \mathbf{q}(\hat{\mathbf{x}})}{\partial t_2}(t_1,t_2)\\ &\quad\doteq \sum_{j_1=-p_1}^{p_1}\sum_{j_2=-p_2}^{p_2} i(\omega_1 j_1 + \omega_2 j_2)\hat{\mathbf{Q}}_{j_1,j_2}(\hat{\mathbf{X}})\exp\left(i(\omega_1 j_1 t_1 + \omega_2 j_2 t_2)\right)\end{aligned} \tag{2.27}$$

and we define the coefficients

$$\hat{\mathbf{H}}_{j_1,j_2}(\hat{\mathbf{X}}) := i(\omega_1 j_1 + \omega_2 j_2)\hat{\mathbf{Q}}_{j_1,j_2}(\hat{\mathbf{X}}) - \hat{\mathbf{F}}_{j_1,j_2}(\hat{\mathbf{X}}). \tag{2.28}$$

https://doi.org/10.1017/S0956792507007188 Published online by Cambridge University Press

Following the Galerkin approach, we employ the test functions

$$\boldsymbol{\Psi}(t_1, t_2) = \mathbf{e} \cdot \exp\left(i(\omega_1 j_1^* t_1 + \omega_2 j_2^* t_2)\right) \tag{2.29}$$

for $j_1^* = -p_1, \ldots, p_1,\ j_2^* = -p_2, \ldots, p_2$, where $\mathbf{e} \in \mathbb{C}^k$ denotes $\mathbf{e} := (1, \ldots, 1)^\top$. Inserting the residual, which depends on the coefficients (2.28), and the test functions in (2.25) yields the equations

$$\begin{aligned} &\frac{1}{T_1 T_2} \int_0^{T_1} \int_0^{T_2} \sum_{j_1=-p_1}^{p_1} \sum_{j_2=-p_2}^{p_2} \hat{\mathbf{H}}_{j_1,j_2}(\hat{\mathbf{X}}) \exp\left(i\tilde{\omega}(t_1, t_2)\right)\, \mathrm{d}t_2\, \mathrm{d}t_1 = \mathbf{0} \\ &\text{with} \quad \tilde{\omega}(t_1, t_2) := \omega_1(j_1 - j_1^*)t_1 + \omega_2(j_2 - j_2^*)t_2 \end{aligned} \tag{2.30}$$

for $j_1^* = -p_1, \ldots, p_1,\ j_2^* = -p_2, \ldots, p_2$. If we interchange integration and summation, then the orthogonality of the basis functions implies

$$\hat{\mathbf{H}}_{j_1,j_2}(\hat{\mathbf{X}}) = \mathbf{0} \quad \text{for} \quad j_1 = -p_1, \ldots, p_1,\ j_2 = -p_2, \ldots, p_2. \tag{2.31}$$

We obtain a non-linear system of $(2p_1 + 1)(2p_2 + 1)k$ equations for the unknown Fourier coefficients in (2.26). Methods of Newton type yield a corresponding approximation of the involved coefficients. The efficient evaluation of the non-linear system and its Jacobian matrix demands discrete Fourier transformations and their inverse mappings. Since we consider solutions $\hat{\mathbf{x}} : \mathbb{R}^2 \to \mathbb{R}^k$, an equivalent real-valued formulation of the approach leads to a non-linear system for the real degrees of freedom only.

The above method has been successfully used in numerical simulations of electric circuits (see [2]). The frequency domain technique is efficient if the time scales exhibit a nearly linear behaviour, i.e., occurring functions are similar to harmonic oscillations. However, strongly non-linear functions in the MPDAE system may demand a huge number of coefficients in the sum (2.26) in order to obtain sufficiently accurate approximations. Hence, the pure frequency domain method becomes inefficient. In this case, time domain techniques offer an adequate alternative.

2.2.2 *Time domain methods*

In time domain, techniques can be applied for solving initial-boundary value problems (2.12) as well as biperiodic boundary value problems (2.11). Finite difference schemes constitute a simple approach for the approximation of biperiodic solutions of the MPDAE (2.10). Thereby, the partial derivatives are replaced by difference formulae using values of the solution on a grid in the time domain. For simplicity, we apply a uniform grid with the points

$$\left(t_{1,j_1}, t_{2,j_2}\right) := ((j_1 - 1)h_1, (j_2 - 1)h_2), \quad \text{where } h_1 := \frac{T_1}{n_1} \text{ and } h_2 := \frac{T_2}{n_2} \tag{2.32}$$

for $j_1 = 1, \ldots, n_1$ and $j_2 = 1, \ldots, n_2$. The values $\hat{\mathbf{x}}_{j_1,j_2} := \hat{\mathbf{x}}(t_{1,j_1}, t_{2,j_2}) \in \mathbb{R}^k$ are unknown. If we substitute the partial derivatives by symmetric differences, for example, we obtain the

https://doi.org/10.1017/S0956792507007188 Published online by Cambridge University Press

non-linear equations

$$\frac{1}{2h_1}\left[\mathbf{q}\left(\hat{\mathbf{x}}_{j_1+1,j_2}\right)-\mathbf{q}\left(\hat{\mathbf{x}}_{j_1-1,j_2}\right)\right]+\frac{1}{2h_2}\left[\mathbf{q}\left(\hat{\mathbf{x}}_{j_1,j_2+1}\right)-\mathbf{q}\left(\hat{\mathbf{x}}_{j_1,j_2-1}\right)\right] \\ =\mathbf{f}\left(\hat{\mathbf{b}}\left(t_{1,j_1},t_{2,j_2}\right),\hat{\mathbf{x}}_{j_1,j_2}\right) \tag{2.33}$$

for $j_1 = 1,\ldots,n_1$ and $j_2 = 1,\ldots,n_2$. The values $\hat{\mathbf{x}}_{j_1,j_2}$ for the indices $j_1 = 0, n_1+1$ and $j_2 = 0, n_2+1$, which are located outside the grid, are identified with the solution inside the grid using the periodicities. This results in a non-linear system of $n_1 n_2 k$ equations for $n_1 n_2 k$ unknowns. Finite difference methods have been successfully used for investigating RF circuits (see [21, 25, 33]).

Considering initial-boundary value problems (2.12), techniques based on semidiscretisation become feasible. Consequently, only one partial derivative in (2.10) is replaced by a difference formula and, thus, a system of DAEs for the resulting approximation needs to be solved. Two types of semidiscretisation techniques exist, which correspond to the method of lines and the Rothe method in case of parabolic PDEs with initial-boundary conditions.

First of all, we consider the technique proceeding similarly to the method of lines. The unknown functions are

$$\tilde{\mathbf{x}}_{j_2}(t_1) := \hat{\mathbf{x}}(t_1,(j_2-1)h_2) \quad \text{with} \quad h_2 := \frac{T_2}{n_2} \quad \text{for} \quad j_2 = 1,\ldots,n_2. \tag{2.34}$$

The partial derivative with respect to the second time scale is replaced by a difference formula. For example, using symmetric differences again, we obtain the discretised systems

$$\frac{\mathrm{d}\mathbf{q}(\tilde{\mathbf{x}}_{j_2})}{\mathrm{d}t_1}(t_1)=\mathbf{f}(\hat{\mathbf{b}}(t_1,(j_2-1)h_2),\tilde{\mathbf{x}}_{j_2}(t_1))-\frac{1}{2h_2}\left[\mathbf{q}(\tilde{\mathbf{x}}_{j_2+1}(t_1))-\mathbf{q}(\tilde{\mathbf{x}}_{j_2-1}(t_1))\right] \tag{2.35}$$

for $j_2 = 1,\ldots,n_2$. The periodicity of the second time scale allows the identification $\tilde{\mathbf{x}}_0 = \tilde{\mathbf{x}}_{n_2}$ and $\tilde{\mathbf{x}}_{n_2+1} = \tilde{\mathbf{x}}_1$. The condition (2.12) yields according initial values at $t_1 = 0$. Thus, we obtain an initial value problem of $n_2 k$ DAEs for the unknown approximations (2.34).

The second approach is based on the Rothe method; i.e., we discretise the derivative with respect to the first time scale. Using equidistant step size h_1, the unknown approximations read

$$\tilde{\mathbf{x}}_{j_1}(t_2) := \hat{\mathbf{x}}((j_1-1)h_1,t_2) \quad \text{for} \quad j_1 = 1,2,3,\ldots. \tag{2.36}$$

For simplicity, we apply a finite difference formula of first order and obtain the systems

$$\frac{\mathrm{d}\mathbf{q}(\tilde{\mathbf{x}}_{j_1})}{\mathrm{d}t_2}(t_2)=\mathbf{f}(\hat{\mathbf{b}}((j_1-1)h_1,t_2),\tilde{\mathbf{x}}_{j_1}(t_2))-\frac{1}{h_1}\left[\mathbf{q}(\tilde{\mathbf{x}}_{j_1}(t_2))-\mathbf{q}(\tilde{\mathbf{x}}_{j_1-1}(t_2))\right] \tag{2.37}$$

for $j_1 = 2,3,\ldots$, where the periodicity of the second time scale implies the boundary conditions $\tilde{\mathbf{x}}_{j_1}(0) = \tilde{\mathbf{x}}_{j_1}(T_2)$ for each j_1. The initial conditions from (2.12) determine the starting function $\tilde{\mathbf{x}}_1$ at $t_1 = 0$. This approach yields a sequence of boundary value problems of k DAEs, which have to be solved successively. In later steps, BDF (backward difference formula) schemes of higher order can be used in the semidiscretisation to improve the accuracy.

https://doi.org/10.1017/S0956792507007188 Published online by Cambridge University Press

Moreover, we can apply the presented techniques based on semidiscretisation to solve the biperiodic problem (2.11). In the first approach, the periodicity in t_1 yields boundary conditions for the DAE systems (2.35) specified by

$$\tilde{\mathbf{x}}_{j_2}(0) = \tilde{\mathbf{x}}_{j_2}(T_1) \quad \text{for all} \quad j_2 = 1, \ldots, n_2. \tag{2.38}$$

This periodic problem can, for example, be solved by methods described in [18]. When applying the second strategy, the periodicity in t_1 imposes

$$\tilde{\mathbf{x}}_1(t_2) = \tilde{\mathbf{x}}_{n_1}(t_2) \quad \text{for all} \quad t_2 \in [0, T_2], \quad \text{where} \quad h_1 := \frac{T_1}{n_1}. \tag{2.39}$$

Since the approximation $\tilde{\mathbf{x}}_{n_1}$ is computed starting from $\tilde{\mathbf{x}}_1$, a condition for the unknown initial values of the biperiodic solution is obtained. Using this approach corresponds to a hierarchical solution of boundary value problems. We try to satisfy the outer condition (2.39) iteratively, whereas we consider the successive inner problems (2.37) to evaluate the outer condition. Numerical results using the latter approach are presented in [24, 33], for example.

The transport of information in the MPDAE system can be used to construct methods of characteristics. Considering the initial-boundary value problem (2.12), we apply a discretisation of the initial manifold. For example, using equidistant step sizes yields the points

$$(t_1, t_2) = (0, (j_2 - 1)h_2) \quad \text{for} \quad h_2 := \frac{T_2}{n_2} \quad \text{and} \quad j_2 = 1, \ldots, n_2. \tag{2.40}$$

A unique characteristic projection runs through each point and the systems according to (2.15) with $\tilde{\mathbf{x}}_{j_2}(\tau) := \hat{\mathbf{x}}(\tau, \tau + (j_2 - 1)h_2)$ are

$$\frac{\mathrm{d}\mathbf{q}(\tilde{\mathbf{x}}_{j_2})}{\mathrm{d}\tau}(\tau) = \mathbf{f}(\hat{\mathbf{b}}(\tau, \tau + (j_2 - 1)h_2), \tilde{\mathbf{x}}_{j_2}(\tau)) \quad \text{for} \quad j_2 = 1, \ldots, n_2. \tag{2.41}$$

Each DAE system can be solved separately for $\tau \in [0, T_1]$, where the end point T_1 is not necessarily a period. The condition (2.12) defines the initial values for the integration. Moreover, the resulting functions represent exact values of the corresponding solution. However, solving a system of the form (2.41) in the complete time interval $[0, T_1]$ for some $T_1 \gg T_2$ demands the same computational effort as an initial value problem of the original DAE (1.1), which should be avoided due to the huge number of oscillations. For example, if $T_1 \approx qT_2$ with $q \gg 1$ holds, then $n_2 q$ oscillations have to be resolved. Hence, although feasible, this approach is drastically inefficient for solving initial-boundary value problems.

Nevertheless, an efficient method of characteristics can be provided in case of biperiodic boundary value problems. Thereby, we exploit the fact that the biperiodic solution is uniquely defined by its initial values on the manifold $\{(t_1, t_2) \in \mathbb{R}^2 : t_2 = 0\}$. Thus, the initial points

$$(t_1, t_2) = ((j_1 - 1)h_1, 0) \quad \text{for} \quad h_1 := \frac{T_1}{n_1} \quad \text{and} \quad j_1 = 1, \ldots, n_1 \tag{2.42}$$

https://doi.org/10.1017/S0956792507007188 Published online by Cambridge University Press

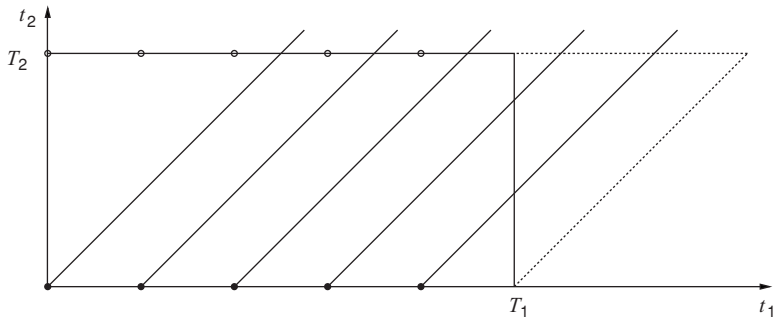

FIGURE 2. Characteristic projections of MPDAE in domain of dependence.

are used. The corresponding systems (2.15) with $\tilde{\mathbf{x}}_{j_1}(\tau) := \hat{\mathbf{x}}(\tau + (j_1 - 1)h_1, \tau)$ read

$$\frac{\mathrm{d}\mathbf{q}(\tilde{\mathbf{x}}_{j_1})}{\mathrm{d}\tau}(\tau) = \mathbf{f}(\hat{\mathbf{b}}(\tau + (j_1 - 1)h_1, \tau), \tilde{\mathbf{x}}_{j_1}(\tau)) \quad \text{for } j_1 = 1, \dots, n_1. \tag{2.43}$$

Now, the advantage is that each system has to be solved only for $\tau \in [0, T_2]$. Since we assume that $T_1 \gg T_2$, only n_1 oscillations have to be captured in each solution of an initial value problem corresponding to the n_1 subsystems (2.43). Again, the systems can be solved separately.

The initial values of the biperiodic solution are unknown a priori. The following strategy can be used to determine these quantities. The periodicity in the first time scale is satisfied via an identification at the boundaries. The periodicity in the second time scale demands

$$\tilde{\mathbf{x}}_{j_1}(0) = \hat{\mathbf{x}}((j_1 - 1)h_1, 0) = \hat{\mathbf{x}}((j_1 - 1)h_1, T_2). \tag{2.44}$$

A unique characteristic projection runs through each initial point as depicted in Figure 2. Solving the systems (2.43) with initial values from the biperiodic solution yields final values on the line $t_2 = T_2$. We apply these values to interpolate the solution in the points $((j_1 - 1)h_1, T_2)$ for $j_1 = 1, \dots, n_1$. The periodicity in the first time variable allows to shift the final values for approximating all given points. Considering (2.44), we obtain the linear boundary conditions

$$(\tilde{\mathbf{x}}_1(0), \dots, \tilde{\mathbf{x}}_{n_1}(0))^\top = \mathscr{B}(\tilde{\mathbf{x}}_1(T_2), \dots, \tilde{\mathbf{x}}_{n_1}(T_2))^\top, \tag{2.45}$$

where $\mathscr{B} \in \mathbb{R}^{n_1 k \times n_1 k}$ represents a constant matrix depending on the used interpolation scheme. Alternatively, a similar condition can be constructed by interpolating the final values of the integration using the initial points. Hence, we end up with a boundary value problem of the $n_1 k$ DAEs (2.43). Solving the problem (2.43), (2.45) yields an approximation of the biperiodic solution in the according parallelogram (see Figure 2). Using the periodicities, we can interpolate an approximation everywhere. The boundary value problem of DAEs can now be solved by shooting methods or finite difference schemes.

The efficiency of this approach results from applying the specific structure of the hyperbolic PDAE system. The separate characteristic systems (2.43) are only coupled by the boundary conditions (2.45). In contrast, a finite difference method based on a uniform

https://doi.org/10.1017/S0956792507007188 Published online by Cambridge University Press

grid performs an unnecessarily strong coupling in both coordinate directions. Thus, concerning the computational effort, the method of characteristics is much more efficient than the standard techniques. A comparison between finite difference methods using on the one hand a uniform grid and on the other hand a characteristic grid is given in [25]. Furthermore, the method of characteristics features an inherent potential for parallelism (see [26]). Even applied to circuits including digital-like signal structures, the method of characteristics constitutes an efficient tool for the numerical simulation (see [17]).

2.2.3 *Mixed domain methods*

In Section 2.2.1, a pure frequency domain method is discussed, which is efficient for mildly non-linear functions in the MPDAE. Otherwise, time domain methods are more preferable. In some applications, the fast time scale behaves nearly linearly, whereas strong non-linearities occur in the slow part. An early idea of Ngoya and Larchevegue [23] is to transform only the second time scale, which is always assumed to be periodic, into the frequency domain. From this approach, we obtain the expansion

$$\hat{\mathbf{x}}(t_1, t_2) \doteq \sum_{j_2=-p_2}^{p_2} \hat{\mathbf{X}}_{j_2}(t_1) \exp(i\omega_2 j_2 t_2) \tag{2.46}$$

with $\hat{\mathbf{X}}_{j_2} : \mathbb{R} \to \mathbb{C}^k$ and $\omega_2 := 2\pi/T_2$. Let $\hat{\mathbf{Q}}_{j_2}(t_1)$ and $\hat{\mathbf{F}}_{j_2}(t_1)$ be the Fourier coefficients of the periodic functions $\mathbf{q}(\hat{\mathbf{x}}(t_1, \cdot))$ and $\mathbf{f}(\hat{\mathbf{b}}(t_1, \cdot), \hat{\mathbf{x}}(t_1, \cdot))$, respectively. These values depend on the unknown functions $\hat{\mathbf{X}} := (\hat{\mathbf{X}}_{j_2}(t_1))$ in (2.46). Following a Galerkin approach similar to the procedure in Section 2.2.1, we obtain the relation

$$\sum_{j_2=-p_2}^{p_2} \left[\frac{\mathrm{d}\hat{\mathbf{Q}}_{j_2}(\hat{\mathbf{X}})}{\mathrm{d}t_1}(t_1) + i\omega_2 j_2 (\hat{\mathbf{Q}}_{j_2}(\hat{\mathbf{X}}))(t_1) - (\hat{\mathbf{F}}_{j_2}(\hat{\mathbf{X}}))(t_1) \right] \exp(i\omega_2 j_2 t_2) = \mathbf{0}. \tag{2.47}$$

Since the occurring basis functions are orthogonal, we obtain the conditions

$$\frac{\mathrm{d}\hat{\mathbf{Q}}_{j_2}(\hat{\mathbf{X}})}{\mathrm{d}t_1}(t_1) = (\hat{\mathbf{F}}_{j_2}(\hat{\mathbf{X}}))(t_1) - i\omega_2 j_2 (\hat{\mathbf{Q}}_{j_2}(\hat{\mathbf{X}}))(t_1) \quad \text{for} \quad j_2 = -p_2, \ldots, p_2, \tag{2.48}$$

representing a system of DAEs for the $(2p_2 + 1)k$ unknown functions $\hat{\mathbf{X}}_{j_2}$. An equivalent real-valued formulation can also be derived. We are now able to use time domain methods for solving this system. Such mixed techniques are feasible, since the time scales are decoupled. Thus, we can tailor our method according to the behaviour of the separate time variables and obtain a mixed time-frequency domain scheme. The initial-boundary value problem (2.12) yields an initial value problem for the resulting DAEs (2.48). A modification of this MPDAE approach has been used in [1, 4] to determine periodic responses of autonomous DAEs (1.1) as well as their a priori unknown periods. On the other hand, the biperiodic boundary value problem (2.11) implies a periodic boundary value problem for the DAEs (2.48). Corresponding numerical simulations are given in [3, 32, 33].

In the above approach, we perform the transformation in the frequency domain first and then apply time domain schemes. Vice versa, mixed methods also result by considering

https://doi.org/10.1017/S0956792507007188 Published online by Cambridge University Press

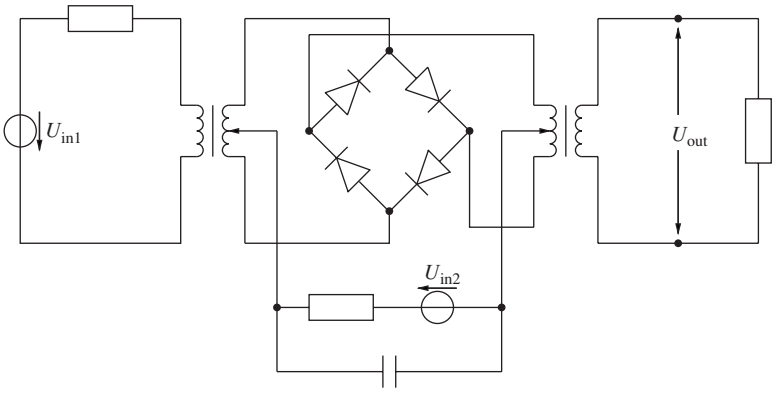

FIGURE 3. Circuit diagram of the ring modulator.

the scheme (2.37), which is resulting from a semidiscretisation in the time domain. The according sequence of periodic boundary value problems of DAEs can also be solved by harmonic balance, i.e., a method in frequency domain. Furthermore, the periodic boundary value problem of the DAEs (2.35) allows the use of frequency domain methods, which may be advantageous in case of a mildly non-linear slow time scale.

2.3 Illustrative example: Ring modulator

As an example for a numerical simulation using the MPDAE model, we consider the ring modulator. Figure 3 shows the corresponding circuit diagram. The ring modulator performs a multiplicative mixture of two independent input signals U_{IN1} and U_{IN2}. A mathematical model of the circuit is introduced by Horneber [14], where an artifical capacitance C_S has been added. Consequently, the model is a system of ordinary differential equations (ODEs) for seven node voltages and eight branch currents:

$$
\begin{aligned}
C\dot{U}_1 &= I_1 - I_3/2 + I_4/2 + I_7 - U_1/R,\\
C\dot{U}_2 &= I_2 - I_5/2 + I_6/2 + I_8 - U_2/R,\\
C_S\dot{U}_3 &= I_3 - d(U_{D1}) + d(U_{D4}),\\
C_S\dot{U}_4 &= -I_4 + d(U_{D2}) - d(U_{D3}),\\
C_S\dot{U}_5 &= I_5 + d(U_{D1}) - d(U_{D3}),\\
C_S\dot{U}_6 &= -I_6 - d(U_{D2}) + d(U_{D4}),\\
C_P\dot{U}_7 &= -U_7/R_P + d(U_{D1}) + d(U_{D2}) - d(U_{D3}) - d(U_{D4}),\\
L_H\dot{I}_1 &= -U_1,\\
L_H\dot{I}_2 &= -U_2,\\
L_{S2}\dot{I}_3 &= U_1/2 - U_3 - R_{G2}I_3,\\
L_{S3}\dot{I}_4 &= -U_1/2 + U_4 - R_{G3}I_4,\\
L_{S2}\dot{I}_5 &= U_2/2 - U_5 - R_{G2}I_5,\\
L_{S3}\dot{I}_6 &= -U_2/2 + U_6 - R_{G3}I_6,\\
L_{S1}\dot{I}_7 &= -U_1 + U_{\text{IN1}} - (R_J + R_{G1})I_7,\\
L_{S1}\dot{I}_8 &= -U_2 - (R_C + R_{G1})I_8.
\end{aligned}
\tag{2.49}
$$

https://doi.org/10.1017/S0956792507007188 Published online by Cambridge University Press

In this system, the following abbreviations for the voltages corresponding to the diodes are used:

$$\begin{aligned} U_{D1} &= U_3 - U_5 - U_7 - U_{\mathrm{IN2}}, & U_{D3} &= U_4 + U_5 + U_7 + U_{\mathrm{IN2}}, \\ U_{D2} &= -U_4 + U_6 - U_7 - U_{\mathrm{IN2}}, & U_{D4} &= -U_3 - U_6 + U_7 + U_{\mathrm{IN2}}. \end{aligned} \tag{2.50}$$

The current–voltage relation of the diodes reads

$$I = d(U) := \gamma(\exp(\delta U) - 1). \tag{2.51}$$

The artificial capacitance C_S causes a parasitic oscillation and, therefore, we set $C_S = 0$ in our simulations. Consequently, the system (2.49) represents a DAE of index 2. More information concerning the mathematical model of the ring modulator is given in [15].

For the input signals, we choose two harmonic oscillations with different periods

$$U_{\mathrm{IN1}}(t) = A_1 \sin\left(\frac{2\pi}{T_1}t\right) \quad \text{and} \quad U_{\mathrm{IN2}}(t) = A_2 \sin\left(\frac{2\pi}{T_2}t\right), \tag{2.52}$$

where $T_1 > T_2$ holds. The output voltage U_{OUT} of the circuit is U_2. Since the ring modulator produces a multiplicative mixture of the input signals, we expect roughly

$$U_{\mathrm{OUT}}(t) \approx B \cdot \sin\left(\frac{2\pi}{T_1}t + \varphi_1\right) \cdot \sin\left(\frac{2\pi}{T_2}t + \varphi_2\right); \tag{2.53}$$

i.e., a multirate behaviour with two separate time scales occurs. Consequently, we change from the DAE system (2.49) to the corresponding MPDAE system of the form (2.10).

The values of the involved parameters are chosen as follows:

$$\begin{aligned} &R_{G1} = 36.3\ \Omega,\ R_{G2} = R_{G3} = 17.3\ \Omega,\ R_J = R_P = 50\ \Omega,\ R_C = 600\ \Omega,\ R = 25\ \mathrm{k}\Omega, \\ &C = 16\ \mathrm{nF},\ C_P = 10\ \mathrm{nF},\ L_H = 4.45\ \mathrm{H},\ L_{S1} = 2\ \mathrm{mH},\ L_{S2} = L_{S3} = 0.5\ \mathrm{mH}, \\ &\gamma = 40.67286402 \cdot 10^{-9}\ \mathrm{A},\ \delta = 17.7493332\mathrm{V}^{-1},\ A_1 = 0.5\ \mathrm{V},\ A_2 = 2\ \mathrm{V}. \end{aligned}$$

The numerical simulation follows [27]. We apply the method of characteristics presented in Section 2.2.2. Thereby, the related boundary value problem (2.43), (2.45) is solved via a finite difference method using a scheme of Dahlquist (see [10]). Although Dahlquist's formula is unstable for solving initial value problems of ODEs, the discretisation of boundary value problems is successful. Furthermore, we use linear interpolation for evaluating the boundary conditions. We fix the slow rate at $T_1 = 1{,}000$ ms, whereas four different cases with respect to the fast rate T_2 are simulated. Figure 4 illustrates the resulting MVFs for the output voltage. The multidimensional model allows a graphic comparison of the signal's behaviour in the time domain. Further numerical simulations using the MPDAE model for a ring modulator circuit are given in [2, 3, 19].

Finally, we use the solution of the MPDAE to reconstruct the corresponding DAE solution via (2.7) in the case $T_1 = 1{,}000$ ms and $T_2 = 0.1$ ms. Consequently, the MVFs allow to reconstruct 10,000 oscillations during one slow period. For comparison, an initial value problem of the DAE (2.49) is solved applying the RADAU5 integrator (see [11]), where the solution of the MPDAE in $t_1 = t_2 = 0$ provides the starting values. Figure 5

https://doi.org/10.1017/S0956792507007188 Published online by Cambridge University Press

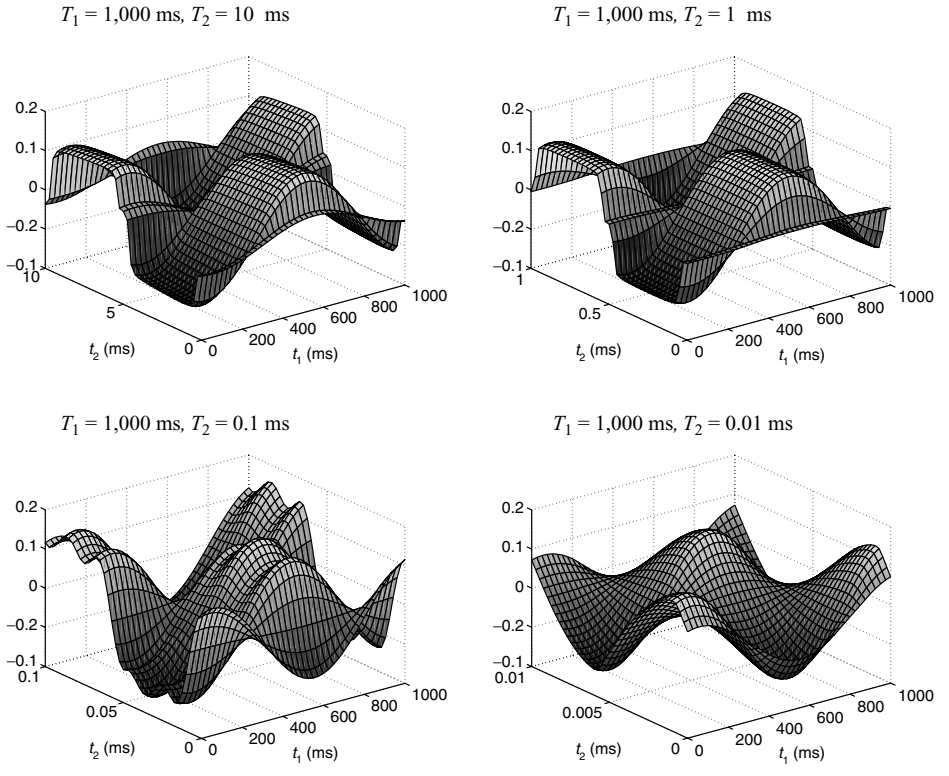

FIGURE 4. MPDAE solutions for $\hat{U}_{\mathrm{OUT}}$ using different time scales.

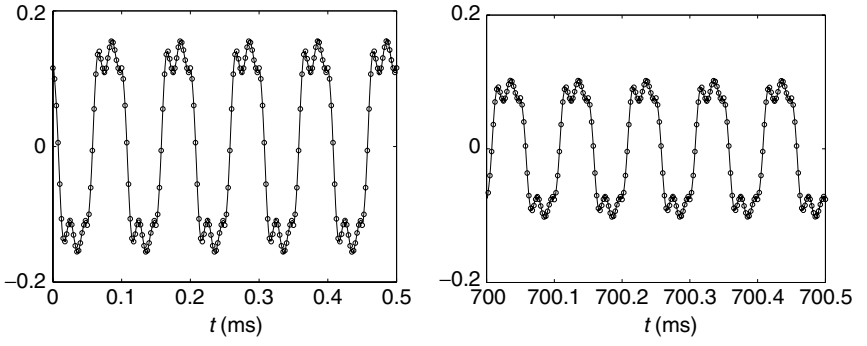

FIGURE 5. Output voltage U_{OUT} obtained by transient analysis of the DAE (solid line) and by reconstruction using the MVF (circles) in time intervals (0 ms, 0.5 ms) and (700 ms, 700.5 ms).

demonstrates the results for two different time intervals. We observe a good agreement of both approximations. In particular, the amplitude modulation is resolved correctly.

The above test example exhibits a medium-sized dimension. Numerical simulations using electric circuits, where the number of unknown voltages and currents is larger, are presented in [20]. For huge dimensions, the non-linear systems for biperiodic problems may become too costly. However, extremely large circuits with the considered multitone

https://doi.org/10.1017/S0956792507007188 Published online by Cambridge University Press

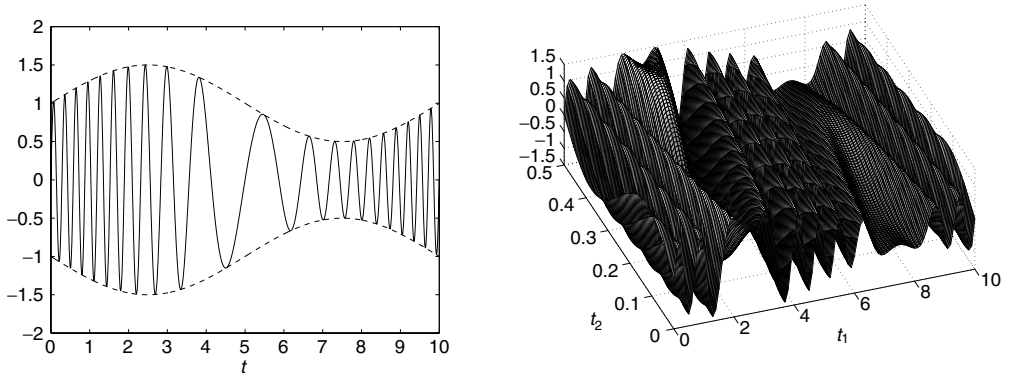

FIGURE 6. Frequency modulated signal x (left) and corresponding naive MVF $\hat{x}$ (right).

behaviour are not likely to appear in practice, since each voltage or current has to feature oscillations of the same time scales. In case of parts with different time behaviour in a circuit, according decompositions are required.

3 Model for frequency modulation

Now, we assume the existence of autonomous parts in an RF circuit, which enable the generation of frequency modulation. Thus, we have to modify the signal model as well as the corresponding MPDAE system to tackle this problem efficiently. Although the succession of the survey is analogue to the previous chapter, the analytical and numerical properties of the multivariate model become different and require a deeper investigation.

3.1 Multidimensional approach

3.1.1 *Multivariate model for AM/FM signals*

In this section, we consider the presence of frequency modulation in addition to amplitude modulation. For example, the multitone signal

$$x(t) := \left[1 + \alpha \sin\left(\frac{2\pi}{T_1} t\right)\right] \cdot \sin\left(\frac{2\pi}{T_2} t + \beta \sin\left(\frac{2\pi}{T_1} t\right)\right) \tag{3.1}$$

with $T_1 \gg T_2$ includes amplitude modulation introduced by the parameter $0 < \alpha < 1$, whereas the parameter $\beta > 0$ determines the amount of frequency modulation. Figure 6 (left) shows the qualitative behaviour of the signal (3.1). We can directly specify a corresponding biperiodic MVF via

$$\hat{x}(t_1, t_2) := \left[1 + \alpha \sin\left(\frac{2\pi}{T_1} t_1\right)\right] \cdot \sin\left(\frac{2\pi}{T_2} t_2 + \beta \sin\left(\frac{2\pi}{T_1} t_1\right)\right). \tag{3.2}$$

Again, the reconstruction reads $x(t) = \hat{x}(t, t)$. Unfortunately, this MVF includes many oscillations in the related rectangle $[0, T_1] \times [0, T_2]$; see Figure 6 (right). The number of oscillations increases the larger the parameter β becomes. The naive representation (3.2)

https://doi.org/10.1017/S0956792507007188 Published online by Cambridge University Press

is inefficient in the case of frequency modulated signals, although it is suitable for purely amplitude modulated signals.

To obtain an appropriate formulation, Narayan and Roychowdhury [22] propose to model the frequency modulation separately. Accordingly, the MVF just includes the amplitude modulation part, which yields the biperiodic description

$$\hat{y}(t_1, t_2) := \left[1 + \alpha \sin\left(\frac{2\pi}{T_1} t_1\right)\right] \cdot \sin(2\pi t_2), \tag{3.3}$$

where the second period is transformed to 1. The alternative MVF (3.3) exhibits the same form as the MVF (2.4) shown in Figure 1 (right). Thus, we again obtain a simple and efficient representation. The frequency modulation part is specified by the additional time-dependent function

$$\Psi(t) := \frac{t}{T_2} + \frac{\beta}{2\pi} \sin\left(\frac{2\pi}{T_1} t\right). \tag{3.4}$$

We perform the reconstruction of the original signal (3.1), using

$$x(t) = \hat{y}(t, \Psi(t)). \tag{3.5}$$

Thereby, the function (3.4) stretches the second time scale and, thus, it is called a *warping function*. The derivative of the warping function can be seen as a *local frequency* of the respective signal. In our example, the local frequency is given by

$$v(t) := \Psi'(t) = \frac{1}{T_2} + \frac{\beta}{T_1} \cos\left(\frac{2\pi}{T_1} t\right), \tag{3.6}$$

which represents a simple T_1-periodic function in time. Hence, we obtain an efficient multidimensional model for frequency modulated signals by means of an MVF and a corresponding local frequency function. Note that the multivariate representation is not unique here, since a family of MVFs and respective local frequencies can reproduce the same signal.

The outlined multidimensional model can be generalised to an arbitrary finite number of time scales. As we have seen in the above example, the signal (3.1) can be described by the MVF (3.2) with constant frequency as well as by the MVF (3.3) including a varying frequency function. We have the choice to arrange a time scale either with a constant frequency or with varying frequency in the multivariate representation. The suitable way of modelling follows from the structure of the underlying signal.

3.1.2 *Warped MPDAE model*

If the solution of the DAE (1.1) exhibits frequency modulation, then the multivariate representation again implies an MPDAE. Narayan and Roychowdhury [22] introduce a corresponding system of *warped multirate partial differential algebraic equations*. In the

https://doi.org/10.1017/S0956792507007188 Published online by Cambridge University Press

general case of m separate time scales, the system reads

$$\sum_{l=1}^{m} v_l(t_1,\ldots,t_m)\frac{\partial \mathbf{q}(\hat{\mathbf{x}})}{\partial t_l} = \mathbf{f}(\hat{\mathbf{b}}(t_1,\ldots,t_m),\hat{\mathbf{x}}(t_1,\ldots,t_m)), \tag{3.7}$$

where $v_l : \mathbb{R}^m \to \mathbb{R}$ represent local frequency functions for $l = 1,\ldots,m$. Setting $v_l \equiv c_l$ with a constant $c_l \in \mathbb{R}$ means that the lth time scale is assumed to own a constant frequency or an aperiodic behaviour. If the local frequency is not constant, then an appropriate function is often unknown a priori. Hence, the system (3.7) is underdetermined and we need additional conditions to identify adequate local frequencies. Some choices of such conditions will be discussed in Section 3.1.5.

In many applications, the input does not include frequency modulated signals but produces frequency modulation in the output signals. If the MVF $\hat{\mathbf{b}}$ involves (without loss of generality) just the first p variables $t_1,\ldots,t_p$ with $p < m$, then the local frequency functions depend only on the same variables.

In the general case (3.7), there exists no explicit formula for the reconstruction of a corresponding DAE solution. Here, the strategy of reconstruction requires the solution of a system of ordinary differential equations (ODEs), which is analysed in Section 3.1.3.

To solve the system (3.7), initial and boundary conditions have to be specified. The multidimensional approach is efficient only if all fast time scales exhibit a periodic behaviour. Only the slowest time scale may be periodic or aperiodic.

In electric circuits involving frequency modulation, the most common case consists in a forced slow time scale together with an autonomous fast time scale. The input signals operate just at the slow time scale and, thus, do not require a multivariate description. Consequently, the corresponding system of warped MPDAEs has the form

$$\frac{\partial \mathbf{q}(\hat{\mathbf{x}})}{\partial t_1} + v(t_1)\frac{\partial \mathbf{q}(\hat{\mathbf{x}})}{\partial t_2} = \mathbf{f}(\mathbf{b}(t_1),\hat{\mathbf{x}}(t_1,t_2)). \tag{3.8}$$

Since we assume that the input produces the frequency modulation, the local frequency function depends on the same variable as the input. In this specific case, it is straightforward to reconstruct a solution of the DAE (1.1) via

$$\mathbf{x}(t) = \hat{\mathbf{x}}\left(t, \int_0^t v(s)\,\mathrm{d}s\right), \tag{3.9}$$

which corresponds to the signal model outlined in Section 3.1.1.

The resulting boundary conditions for the warped MPDAE (3.8) are analogous to the case of constant frequencies, cf. Section 2.1.2. If the input signal is aperiodic, then we obtain an initial-boundary value problem (2.12) with $T_2 = 1$. The second period is normalised to 1, whereas the local frequency specifies the magnitude of the second time scale. In case of T_1-periodic input signals, a biperiodic solution of the pure boundary value problem (2.11) with $T_2 = 1$ is to be determined. Furthermore, the discussion from Section 2.1.4 can be performed in an analogous way to verify the well-posedness of the system (3.8).

https://doi.org/10.1017/S0956792507007188 Published online by Cambridge University Press

3.1.3 *Characteristic system of the warped MPDAE*

According to the multirate system (2.6), warped MPDAE systems also exhibit a hyperbolic structure. We obtain a corresponding *characteristic system*, which completely describes the transport of information. The characteristic system of the general warped MPDAE (3.7) reads

$$\begin{aligned} \frac{\mathrm{d}}{\mathrm{d}\tau} t_l(\tau) &= v_l(t_1(\tau), \dots, t_m(\tau)), \quad l = 1, \dots, m, \\ \frac{\mathrm{d}}{\mathrm{d}\tau} \mathbf{q}(\hat{\mathbf{x}}(\tau)) &= \mathbf{f}\left(\mathbf{b}(t_1(\tau), \dots, t_m(\tau)), \hat{\mathbf{x}}(\tau)\right), \end{aligned} \tag{3.10}$$

where the variables t_l as well as the MVF $\hat{\mathbf{x}}$ depend on a parameter τ. For given local frequency functions, the part for the variables $t_1, \dots, t_m$, represents a system of ODEs. A solution of this system yields the *characteristic projections*. If solutions of corresponding initial value problems are always unique, then two different characteristic projections never intersect. For example, the uniqueness can be guaranteed via $v_l \in C^1$ for all l.

In contrast to constant frequencies, we do not have an explicit formula for the characteristic projections in this general case. Considering a specific characteristic projection, we obtain the whole *characteristic curve* by solving the last equation in (3.10), which represents a system of DAEs. The solution of (3.10) with initial values

$$t_1(0) = \cdots = t_m(0) = 0, \quad \hat{\mathbf{x}}(0) = \mathbf{x}_0 \tag{3.11}$$

recovers a solution of the original DAE (1.1). Therefore, solving the ODE part in (3.10) is necessary to obtain the reconstruction scheme for solutions of the underlying DAE.

In the important case (3.8) with two time scales, we obtain the characteristic system

$$\begin{aligned} \frac{\mathrm{d}}{\mathrm{d}\tau} t_1(\tau) &= 1, \\ \frac{\mathrm{d}}{\mathrm{d}\tau} t_2(\tau) &= v(t_1(\tau)), \\ \frac{\mathrm{d}}{\mathrm{d}\tau} \mathbf{q}(\hat{\mathbf{x}}(\tau)) &= \mathbf{f}\left(\mathbf{b}(t_1(\tau)), \hat{\mathbf{x}}(\tau)\right). \end{aligned} \tag{3.12}$$

We are able to solve the part for the variables t_1, t_2 explicitly and we obtain characteristic projections of the form

$$t_2(t_1) = \int_0^{t_1} v(s)\, \mathrm{d}s + c \quad \text{for arbitrary } \; c \in \mathbb{R}, \tag{3.13}$$

which generate a continuum of parallel curves in the domain of dependence.

3.1.4 *Transformation properties*

We can transform an MVF satisfying the general system (3.7) for a specific local frequency function into an MVF fulfilling the system with another local frequency. However, such a transformation is interesting only if it does not change a certain initial manifold. In case of two time scales, an MVF $\hat{\mathbf{x}}$ solving the MPDAE (3.8) for a local frequency function $v \in C^0$ can be transformed to another MVF $\hat{\mathbf{y}}$ satisfying the system with an

https://doi.org/10.1017/S0956792507007188 Published online by Cambridge University Press

arbitrary local frequency $\mu \in C^0$ via

$$\hat{\mathbf{y}}(t_1, t_2) := \hat{\mathbf{x}}\left(t_1, t_2 + \int_0^{t_1} v(s) - \mu(s)\, \mathrm{d}s\right). \tag{3.14}$$

The initial manifold $\{(t_1, t_2) \in \mathbb{R}^2 : t_1 = 0\}$ is invariant under this transformation. In particular, both solutions yield the same solution of the underlying DAE (1.1) in the corresponding reconstructions (3.9), since

$$\mathbf{x}(t) = \hat{\mathbf{x}}\left(t, \int_0^t v(s)\, \mathrm{d}s\right) = \hat{\mathbf{y}}\left(t, \int_0^t \mu(s)\, \mathrm{d}s\right). \tag{3.15}$$

Hence, the local frequencies represent free parameters in the multidimensional approach, which we can specify to achieve an efficient representation by corresponding MVFs. However, we do not have knowledge about the solutions a priori. We need additional conditions, which identify appropriate local frequency functions.

For biperiodic MVFs, the involved local frequency functions have to satisfy some restrictions in order to preserve the periodicities in the transformation (3.14). The four properties

$$\begin{aligned} &\text{(i)} \quad \hat{\mathbf{x}} \in C^1 \text{ is } (T_1, 1)\text{-periodic}, && \text{(iii)} \quad \mu \in C^0 \text{ is } T_1\text{-periodic}, \\ &\text{(ii)} \quad v \in C^0 \text{ is } T_1\text{-periodic}, && \text{(iv)} \quad \textstyle\int_0^{T_1} \mu(s)\, \mathrm{d}s = \int_0^{T_1} v(s)\, \mathrm{d}s, \end{aligned} \tag{3.16}$$

guarantee that the function $\hat{\mathbf{y}} \in C^1$ defined by (3.14) is $(T_1, 1)$-periodic. The requirements (i)–(iii) are obvious. Defining the average frequency of a periodic local frequency function $\sigma \in C^0$ as

$$\overline{\sigma} := \frac{1}{T_1} \int_0^{T_1} \sigma(s)\, \mathrm{d}s, \tag{3.17}$$

property (iv) implies that the average frequencies coincide, i.e., $\overline{v} = \overline{\mu}$. Therefore, the existence of one biperiodic solution yields a family of solutions with the same average frequency generated via (3.14). In particular, a solution corresponding to a constant local frequency $\overline{v}$ exists; i.e., it satisfies a standardised form of the MPDAE (2.10).

Furthermore, the specific system (3.8) is autonomous in the second time scale. Thus, given an MVF satisfying the system, the shifted function

$$\hat{\mathbf{z}}(t_1, t_2) := \hat{\mathbf{x}}(t_1, t_2 + c) \text{ for constant } c \in \mathbb{R} \tag{3.18}$$

represents a solution corresponding to the same local frequency function again. This transformation, which is obvious on the MPDAE level, represents a hidden degree of freedom in solutions of the original DAE system (1.1).

3.1.5 *Additional conditions*

In this section, we discuss the identification of adequate local frequency functions. We restrict ourselves to the case of two time scales described by the system (3.8), where

https://doi.org/10.1017/S0956792507007188 Published online by Cambridge University Press

just one frequency function has to be specified. If widely separated time scales are present, then small changes in the local frequency function cause huge deformations in the corresponding MVFs due to the transformation (3.14) (see [28]). In view of this sensitivity, we cannot expect that an a priori specification of the local frequencies yields a suitable solution. The local frequency function has to be determined indirectly by additional conditions, which use the representation by MVFs.

Narayan and Roychowdhury [22] propose a continuum of *phase conditions*, which control the phase in each cross section of the MVF corresponding to a constant value t_1. Without loss of generality, we choose the first component of the MVF $\hat{\mathbf{x}} = (\hat{x}^1, \dots, \hat{x}^k)^\top$. In time domain, an example for a phase condition reads

$$\hat{x}^1(t_1, 0) = \eta(t_1) \quad \text{for all} \quad t_1 \in \mathbb{R} \tag{3.19}$$

with predetermined function $\eta : \mathbb{R} \to \mathbb{R}$. Appropriate constant choices $\eta \equiv \eta_0$ are often sufficient. Another example is given by

$$\frac{\partial \hat{x}^1}{\partial t_2}(t_1, 0) = \eta(t_1) \quad \text{for all} \quad t_1 \in \mathbb{R}. \tag{3.20}$$

Thereby, it is often appropriate to require $\eta \equiv 0$. The constant choices represent multi-dimensional generalisations of phase conditions for DAEs. Both (3.19) and (3.20) yield an additional boundary condition in the time domain. The existence of corresponding solutions can be motivated by the implicit function theorem and employing the transformations (3.14) and (3.18). We may apply these phase conditions for solving pure boundary value problems (2.11) as well as initial-boundary value problems (2.12).

If the fast time scale is transformed in the frequency domain, then phase conditions can be based on Fourier coefficients of the MVF (see [22]). A simple example is the requirement

$$\mathrm{Im}\big(X_j^1(t_1)\big) = 0 \quad \text{for all} \quad t_1 \in \mathbb{R}, \tag{3.21}$$

where $\mathrm{Im}(X_j^1) : \mathbb{R} \to \mathbb{R}$ represents the imaginary part of the jth coefficient in the Fourier expansion applied to the first component $\hat{x}^1$. Zhu and Christoffersen [38, 39] succeed in using conditions with Fourier coefficients for numerical simulations.

In general, elementary phase conditions already yield simple, i.e., efficient solutions of the MPDAE system. However, this favourable property cannot be proven universally. Therefore, the idea is to incorporate the complete MVF in order to determine an optimal solution. Clearly, the optimality condition still needs to be specified.

Houben [13] introduces a *minimisation criterion* of the form

$$\beta(t_1) := \int_0^1 \left\| \frac{\partial \mathbf{q}(\hat{\mathbf{x}})}{\partial t_1} \right\|^2 \mathrm{d}t_2 \quad \to \quad \min. \quad \text{for each} \quad t_1 \tag{3.22}$$

using the Euclidean norm $\|\cdot\|$ in the space $\mathbb{R}^k$. The function β includes just the derivative with respect to the slow time scale, since the derivative corresponding to the fast time scale is invariant under the transformation (3.14). The example in Section 3.1.1 illustrates

https://doi.org/10.1017/S0956792507007188 Published online by Cambridge University Press

that inappropriate MVFs exhibit many oscillations in the direction of the slow time scale. This disadvantageous behaviour can be improved by requiring (3.22).

An according calculation yields an explicit formula for the optimal local frequencies depending on the MVF, namely

$$\nu_{\mathrm{opt}}(t_1) = \frac{\displaystyle\int_0^1 \left\langle \mathbf{f}\left(\mathbf{b}(t_1), \hat{\mathbf{x}}(t_1,t_2)\right), \frac{\partial \mathbf{q}(\hat{\mathbf{x}})}{\partial t_2} \right\rangle \mathrm{d}t_2}{\displaystyle\int_0^1 \left\| \frac{\partial \mathbf{q}(\hat{\mathbf{x}})}{\partial t_2} \right\|^2 \mathrm{d}t_2}\,, \tag{3.23}$$

where the inner product of the space $\mathbb{R}^k$ is denoted by $< \cdot, \cdot >$. Inserting (3.23) in the MPDAE (3.8) allows for solving the initial-boundary value problems (2.12) directly. However, instead of using the solution $\hat{\mathbf{x}}$ itself, the minimisation is based on the function $\mathbf{q}(\hat{\mathbf{x}})$ to replace corresponding derivatives by terms in (3.8). In many cases, the MVF $\hat{\mathbf{x}}$ will be efficient if and only if $\mathbf{q}(\hat{\mathbf{x}})$ represents a simple function. Yet this property cannot be guaranteed in general. Moreover, considering a semi-explicit DAE for (1.1), the minimisation does not involve the algebraic variables.

Thus, another approach consists in minimising the derivatives of the MVF itself (see [31]). Considering biperiodic boundary value problems (2.11), the corresponding requirement reads

$$\gamma(\hat{\mathbf{x}}) := T_1 \int_0^{T_1} \int_0^1 \sum_{l=1}^{k} w_l \left(\frac{\partial \hat{x}^l}{\partial t_1} \right)^2 \mathrm{d}t_2\, \mathrm{d}t_1 \quad \rightarrow \quad \min. \tag{3.24}$$

with constant weights $w_1, \ldots, w_k \geqslant 0$. The weights can be used to achieve an appropriate scaling in each component if the corresponding physical quantities differ by several orders of magnitude. Moreover, setting some weights to zero allows to focus on an arbitrary subset of components.

Based on the transformation formula (3.14), a corresponding *variational calculus* implies a necessary condition for an optimal solution, namely

$$r(t_1) := \int_0^1 \sum_{l=1}^{k} w_l \cdot \frac{\partial^2 \hat{x}^l}{\partial {t_1}^2} \cdot \frac{\partial \hat{x}^l}{\partial t_2}\, \mathrm{d}t_2 = 0 \quad \text{for all } \; t_1 \in \mathbb{R}\,. \tag{3.25}$$

In contrast to the phase conditions (3.19) and (3.20), the requirement (3.25) is not a boundary condition, but depends on values in the complete biperiodic domain of dependence, which is needed to perform the minimisation everywhere. If an arbitrary biperiodic solution of the MPDAE (3.8) exists, then the existence of an optimal function with respect to the minimisation (3.24) can be expected in the continuum of transformed solutions. In case of initial-boundary value problems (2.12), alternative minimisation criteria imposed on the MVF itself have to be considered.

All presented conditions involve scalar functions depending on the slow time scale. Thus, the structure of an additional requirement always agrees to the amount of free parameters in the problem, since the local frequency function also represents a scalar function depending on the slow time scale.

https://doi.org/10.1017/S0956792507007188 Published online by Cambridge University Press

Furthermore, the existence of a biperiodic solution implies a continuum of biperiodic solutions with the same local frequency function via the translation (3.18). Consequently, for biperiodic boundary value problems (2.11), another extra condition is necessary to isolate a specific solution from the continuum. For this purpose, we may apply scalar phase conditions like

$$\hat{x}^1(0,0) = \eta_0 \quad \text{or} \quad \frac{\partial \hat{x}^1}{\partial t_2}(0,0) = \eta_0 \quad \text{for a constant } \eta_0 \in \mathbb{R}\,. \tag{3.26}$$

In the first variant, the constant η_0 has just to be chosen out of the range of $\hat{x}^1(0,\cdot)$. In the second type, the choice $\eta_0 = 0$ is always feasible, since $\hat{x}^1(0,\cdot)$ is a smooth and periodic function. Employing the continuous phase condition (3.19) or (3.20), this specification is done automatically.

3.2 Numerical methods

In general, we can modify a numerical technique for solving the MPDAE (2.6) to derive a method for solving the warped MPDAE (3.7). We outline these transitions for the methods presented in Section 2.2. Thereby, we consider the system (3.8) with two time scales. Consequently, an additional condition to identify the local frequency function (see Section 3.1.5) has to be included in each scheme.

3.2.1 *Frequency domain methods*

In this section, we sketch the construction of a pure frequency domain method to solve the biperiodic boundary value problem (2.11) of the MPDAE (3.8). Following Section 2.2.1, we apply the finite sum (2.26) with $\omega_2 = 2\pi$ as approximation for the $(T_1, 1)$-periodic MVF. Again the partial derivatives in the MPDAE are given by a modification of the respective coefficients; see (2.27). However, the partial derivative with respect to t_2 is multiplied with the local frequency in the MPDAE. We obtain additional coefficients for the biperiodic function

$$v(t_1)\frac{\partial \mathbf{q}(\hat{\mathbf{x}})}{\partial t_2}(t_1,t_2) \doteq \sum_{j_1=-p_1}^{p_1} \sum_{j_2=-p_2}^{p_2} \hat{\mathbf{R}}_{j_1,j_2}(\hat{\mathbf{X}}, v) \exp\left(i(\omega_1 j_1 t_1 + 2\pi j_2 t_2)\right). \tag{3.27}$$

These values depend on the coefficients $\hat{\mathbf{X}}_{j_1,j_2}$ as well as on the local frequency function, which represents a drawback in frequency domain methods applied to warped MPDAEs in comparison to common MPDAEs. The corresponding Galerkin approach yields the non-linear system

$$\hat{\mathbf{G}}_{j_1,j_2}(\hat{\mathbf{X}}) := i\omega_1 j_1 \hat{\mathbf{Q}}_{j_1,j_2}(\hat{\mathbf{X}}) + \hat{\mathbf{R}}_{j_1,j_2}(\hat{\mathbf{X}}, v) - \hat{\mathbf{F}}_{j_1,j_2}(\hat{\mathbf{X}}) = \mathbf{0} \tag{3.28}$$

for $j_1 = -p_1, \ldots, p_1,\ j_2 = -p_2, \ldots, p_2$. Nevertheless, since the values $\hat{\mathbf{Q}}_{j_1,j_2}(\hat{\mathbf{X}})$ have to be computed to handle the first derivative, these coefficients can be used to evaluate the second derivative in the time domain. Given some T_1-periodic function v, the term on the left-hand side in (3.27) can be transformed to frequency domain.

https://doi.org/10.1017/S0956792507007188 Published online by Cambridge University Press

As usual, the periodic local frequency function is unknown a priori. If a representation of the form

$$v(t_1) = \sum_{j_1=-\infty}^{\infty} N_{j_1} \exp(i\omega_1 j_1 t_1) \tag{3.29}$$

exists and when we choose a finite sum in (3.29), we then need to compute a finite number of unknown coefficients. Furthermore, we may apply an approximation for v by defining a set of T_1-periodic functions, which depend on some parameters. The unknown parameters are determined via additional conditions obtained from phase conditions.

According to Section 2.2.1, an approach in the frequency domain causes a non-linear system for the involved Fourier coefficients. In corresponding Newton methods, the evaluation of the system and its Jacobian matrix has to be done by appropriate transformations between time and frequency domain. Methods of this type have not been used to simulate practical examples of warped MPDAEs yet.

3.2.2 *Time domain methods*

The possibly simplest algorithm to solve biperiodic boundary value problems of the warped MPDAE (3.8) is based on a discretisation of the partial derivatives using a uniform grid in the time domain. This approach corresponds to the finite difference methods presented in Section 2.2.2. According to the problem (2.11), we consider the periods T_1 and $T_2 = 1$. For example, if we employ symmetric differences with respect to the grid (2.32), then we again obtain the non-linear equations

$$\begin{aligned} &\frac{1}{2h_1}\left[\mathbf{q}\left(\hat{\mathbf{x}}_{j_1+1,j_2}\right) - \mathbf{q}\left(\hat{\mathbf{x}}_{j_1-1,j_2}\right)\right] + v_{j_1}\frac{1}{2h_2}\left[\mathbf{q}\left(\hat{\mathbf{x}}_{j_1,j_2+1}\right) - \mathbf{q}\left(\hat{\mathbf{x}}_{j_1,j_2-1}\right)\right] \\ &\quad = \mathbf{f}\left(\mathbf{b}(t_{1,j_1}), \hat{\mathbf{x}}_{j_1,j_2}\right) \end{aligned} \tag{3.30}$$

for $j_1 = 1, \ldots, n_1,\ j_2 = 1, \ldots, n_2$. Thereby, the values

$$v_{j_1} \doteq v\left(t_{1,j_1}\right) \quad \text{for } j_1 = 1, \ldots, n_1 \tag{3.31}$$

represent additional unknowns. This system of $n_1 n_2 k$ equations exhibits $n_1 n_2 k + n_1$ unknowns. To formulate a well-defined discretised problem, further conditions have to be imposed. The phase condition (3.19) yields n_1 additional equations. Likewise, n_1 equations can be obtained by discretising the phase condition (3.20) on the uniform grid.

Furthermore, an appropriate approximation of (3.25) on the uniform grid allows to use the condition from the minimisation criterion (3.24). For example, a straightforward discretisation produces the approximation

$$\begin{aligned} r(t_{1,j_1}) \doteq h_2 \sum_{j_2=1}^{n_2} \sum_{l=1}^{k} w_l \cdot &\frac{1}{{h_1}^2}\left[\hat{x}^l_{j_1-1,j_2} - 2\hat{x}^l_{j_1,j_2} + \hat{x}^l_{j_1+1,j_2}\right] \\ &\cdot \frac{1}{2h_2}\left[\hat{x}^l_{j_1,j_2+1} - \hat{x}^l_{j_1,j_2-1}\right] \qquad = 0 \end{aligned} \tag{3.32}$$

for $j_1 = 1, \ldots, n_1$. Due to the periodicity, only values at the grid points are involved. The

https://doi.org/10.1017/S0956792507007188 Published online by Cambridge University Press

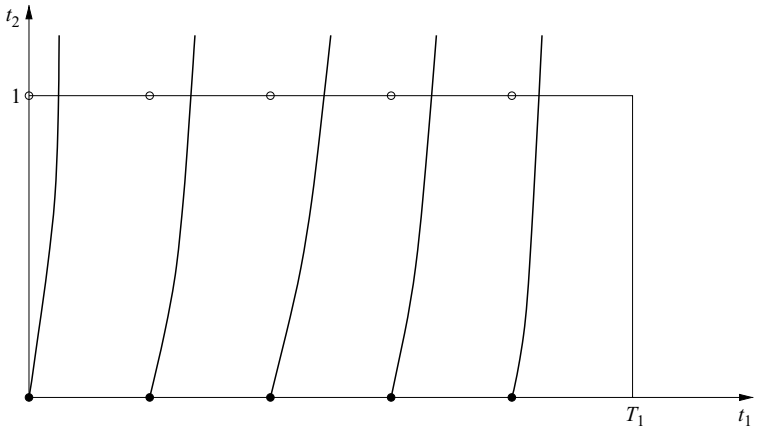

FIGURE 7. Characteristic projections of warped MPDAE in domain of dependence.

computational effort of the method is not significantly higher in comparison to techniques using phase conditions, since the discretisation of the MPDAE system represents the most expensive part of the procedure. Recall that only n_1 conditions are added to a system of $n_1 n_2 k$ equations. Finite difference methods including the additional conditions (3.32) have been successfully used for numerical simulations (see [31]).

In Section 2.2.2, a method of characteristics has been presented for solving biperiodic problems in case of constant frequencies. This approach can be transferred to the warped MPDAE system using the transport of information outlined in Section 3.1.3. However, the construction of the technique becomes more complicated, since the characteristic projections depend on the a priori unknown local frequency. Nevertheless, we obtain an efficient and robust method for solving the biperiodic problem (2.11) (see also [28]).

In the following, we consider widely separated time scales, i.e., $\nu(t_1) \gg T_1^{-1}$ for all t_1. In particular, $\nu \geqslant 0$ holds. As in the previous method of characteristics, we choose the initial points (2.42). According to the characteristic system (3.12), a unique characteristic projection belongs to each initial point given by

$$t_{1,j_1}(\tau) = \tau + (j_1 - 1)h_1, \quad t_{2,j_1}(\tau) = \int_{(j_1-1)h_1}^{(j_1-1)h_1+\tau} \nu(s)\,\mathrm{d}s \quad \text{for } j_1 = 1, \ldots, n_1. \tag{3.33}$$

Figure 7 illustrates the arising characteristic projections. The last equation in (3.12) yields the corresponding characteristic systems for $\tilde{\mathbf{x}}_{j_1}(\tau) := \hat{\mathbf{x}}(t_{1,j_1}(\tau), t_{2,j_1}(\tau))$,

$$\frac{\mathrm{d}\mathbf{q}(\tilde{\mathbf{x}}_{j_1})}{\mathrm{d}\tau}(\tau) = \mathbf{f}\left(\mathbf{b}(\tau + (j_1 - 1)h_1), \tilde{\mathbf{x}}_{j_1}(\tau)\right) \quad \text{for } j_1 = 1, \ldots, n_1. \tag{3.34}$$

The j_1th projection (3.33) intersects the line $t_2 = 1$ in an end point corresponding to the value τ_{j_1}. Since the characteristic projections depend on the frequency function, the n_1 parameters τ_{j_1} are unknown a priori. Again we can use the solution obtained from the DAE systems (3.34) to interpolate the points required for the periodicity condition in the

https://doi.org/10.1017/S0956792507007188 Published online by Cambridge University Press

second time scale. Hence, the resulting boundary conditions exhibit the form

$$(\tilde{\mathbf{x}}_1(0),\dots,\tilde{\mathbf{x}}_{n_1}(0))^\top = \mathscr{B}(\tilde{\mathbf{x}}_1(\tau_1),\dots,\tilde{\mathbf{x}}_{n_1}(\tau_{n_1}))^\top. \tag{3.35}$$

Thereby, the matrix $\mathscr{B} \in \mathbb{R}^{n_1 k \times n_1 k}$ depends on the used interpolation scheme and the unknown parameters $\tau_1,\dots,\tau_{n_1}$.

The selection of the initial points suggests to use the discretisation (3.31) of the local frequency function again. A quadrature scheme generates an approximation of the integrals in (3.33), where we employ exclusively the values from (3.31). For example, in case of largely differing time scales, the trapezoidal rule approximates the j_1th characteristic projection by a quadratic polynomial

$$t_{2,j_1}(\tau) = \int_{(j_1-1)h_1}^{(j_1-1)h_1+\tau} v(s)\,\mathrm{d}s \doteq \left(\tau - \frac{\tau^2}{2h_1}\right) v_{j_1} + \frac{\tau^2}{2h_1} v_{j_1+1} \quad \text{for } \tau \in [0, h_1]. \tag{3.36}$$

If an initial guess for the local frequency is given, we obtain an approximation for the end points $\tau_1,\dots,\tau_{n_1}$ and, thus, we can evaluate the non-linear system (3.35).

The strategy leads to a boundary value problem of DAEs given by (3.34), (3.35). We can solve the problem numerically using shooting methods or finite difference methods, for example. Using the phase conditions, we are able to specify the additional unknowns (3.31). The requirement (3.19) can be added directly to the boundary conditions (3.35), since only initial values are involved. On the other hand, an appropriate discretisation of the demand (3.20) is necessary for achieving a condition, which depends just on the initial values. Both phase conditions have been successfully used in methods of characteristics (see [29]).

The inclusion of requirements from minimisation criteria like (3.32), for example, becomes more difficult, since values of the solution outside the characteristic systems are needed. Nevertheless, if we apply a finite difference method for solving (3.34),(3.35), quantities from a characteristic grid can be interpolated on a uniform grid just to evaluate the conditions (3.32). The use of methods of characteristics involving conditions for optimal solutions is feasible.

For solving initial-boundary value problems (2.12) in the time domain, the construction of techniques based on semidiscretisation is obvious (cf. Section 2.2.2). Houben [13] employs a method of lines to solve the MPDAE (3.8), where the local frequency function is replaced by (3.23). Using phase conditions, the approximate DAE systems from the semidiscretisation have to include an additional algebraic constraint for identifying the frequencies. Theory and numerical behaviour of such techniques are topics of current research. The application of some elementary schemes is investigated in [30].

3.2.3 *Mixed Domain Techniques*

Finally, we briefly discuss the use of mixed time-frequency domain methods for warped MPDAEs. The motivation of these methods is the same as explained in Section 2.2.3. Corresponding techniques are introduced in [22]. The MVF is approximated by the finite

https://doi.org/10.1017/S0956792507007188 Published online by Cambridge University Press

sum (2.46) with $\omega_2 = 2\pi$. Consequently, the MPDAE (3.8) implies the condition

$$\sum_{j_2=-p_2}^{p_2} \left[\frac{\mathrm{d}\hat{\mathbf{Q}}_{j_2}(\hat{\mathbf{X}})}{\mathrm{d}t_1}(t_1) + i2\pi j_2 v(t_1)(\hat{\mathbf{Q}}_{j_2}(\hat{\mathbf{X}}))(t_1) - (\hat{\mathbf{F}}_{j_2}(\hat{\mathbf{X}}))(t_1) \right] \cdot \exp(i2\pi j_2 t_2) = \mathbf{0}, \tag{3.37}$$

where $(\hat{\mathbf{Q}}_{j_2}(\hat{\mathbf{X}}))(t_1)$ and $(\hat{\mathbf{F}}_{j_2}(\hat{\mathbf{X}}))(t_1)$ denote the Fourier coefficients of the functions $\mathbf{q}(\hat{\mathbf{x}}(t_1,\cdot))$ and $\mathbf{f}(\mathbf{b}(t_1), \hat{\mathbf{x}}(t_1,\cdot))$, respectively. Since the basis functions are orthogonal, we obtain the coupled systems

$$\frac{\mathrm{d}\hat{\mathbf{Q}}_{j_2}(\hat{\mathbf{X}})}{\mathrm{d}t_1}(t_1) = (\hat{\mathbf{F}}_{j_2}(\hat{\mathbf{X}}))(t_1) - i2\pi j_2 v(t_1)(\hat{\mathbf{Q}}_{j_2}(\hat{\mathbf{X}}))(t_1), \quad j_2 = -p_2, \ldots, p_2. \tag{3.38}$$

A system of DAEs for the unknown functions in the approximation (2.46) results. Initial or boundary value problems of this system correspond to Section 2.2.3.

However, the local frequency function v is unknown. We obtain a well-defined DAE system by imposing a condition, which involves the Fourier coefficients. For example, requirements like (3.21) directly prescribe the real or imaginary part of an unknown function. Numerical simulations employing conditions with Fourier coefficients are presented in [38, 39]. Moreover, phase conditions defined in the time domain can be transformed into the frequency domain to derive equivalent requirements, which possibly couple all functions.

3.3 Illustrative example: Colpitt oscillator

To simulate a realistic electric circuit again, we examine a forced Colpitt oscillator. The Colpitt oscillator represents a typical LC-oscillator. The circuit includes one inductance, four capacitances and a bipolar transistor (see Figure 8). A specific mathematical model of the Colpitt oscillator leads to an implicit ODE system, which describes the transient behaviour of four node voltages

$$\begin{pmatrix} 1 & 0 & 0 & 0 \\ 0 & C_1 + C_3 & -C_3 & -C_1 \\ 0 & -C_3 & C_2 + C_3 + C_4 & -C_2 \\ 0 & -C_1 & -C_2 & C_1 + C_2 \end{pmatrix} \begin{pmatrix} \dot{U}_1 \\ \dot{U}_2 \\ \dot{U}_3 \\ \dot{U}_4 \end{pmatrix}$$

$$= \begin{pmatrix} \dfrac{R_2}{L}(U_2 - U_1) + R_2 \dot{U}_{op} \\ \dfrac{1}{R_2}(U_{op} - U_1) + \left(I_S + \dfrac{I_S}{b_C} \right) g(U_4 - U_2) - I_S g(U_4 - U_3) \\ -\dfrac{1}{R_4} U_3 + \left(I_S + \dfrac{I_S}{b_E} \right) g(U_4 - U_3) - I_S g(U_4 - U_2) \\ -\dfrac{1}{R_3} U_4 + \dfrac{1}{R_1}(U_{op} - U_4) - \dfrac{I_S}{b_E} g(U_4 - U_3) - \dfrac{I_S}{b_C} g(U_4 - U_2) \end{pmatrix}. \tag{3.39}$$

https://doi.org/10.1017/S0956792507007188 Published online by Cambridge University Press

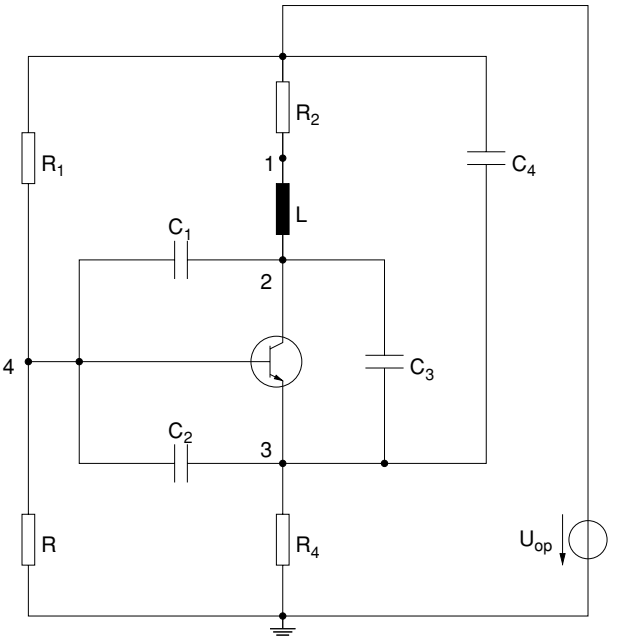

FIGURE 8. Circuit of Colpitt oscillator.

The applied transistor model includes the non-linear function

$$g(U) = \exp\left(\frac{U}{U_T}\right) - 1. \tag{3.40}$$

The values of the technical parameters are set as follows:

$$C_1 = 50 \text{ pF},\ C_2 = 1 \text{ nF},\ C_3 = 50 \text{ nF},\ C_4 = 100 \text{ nF},\ R_1 = 12 \text{ k}\Omega,$$
$$R_2 = 3\ \Omega,\ R_3 = 8.2 \text{ k}\Omega,\ R_4 = 1.5 \text{ k}\Omega,\ L = 10 \text{ mH},\ U_{op} = 10 \text{ V},$$
$$I_S = 1 \text{ mA},\ b_E = 100,\ b_C = 50,\ U_T = 25.85 \text{ mV}.$$

Using these parameters, the Colpitt oscillator has a periodic solution with time rate $T_0 = 0.125$ ms. More details about the modelling of the Colpitt oscillator can be found in [15].

Now, an external source controls the third capacitor

$$\tilde{C}_3(t) = C_3\left(1 + 0.8\sin\left(\frac{2\pi}{T_1}t\right)\right) \tag{3.41}$$

and we choose $T_1 = 1$ s (see Figure 9 (left)). Hence, the capacitance matrix in (3.39) becomes time-dependent and the system is no longer of the form (1.1). Nevertheless, the resulting capacitance matrix is always regular; i.e., the arising system is equivalent to an explicit ODE, which represents a special case of (1.1).

https://doi.org/10.1017/S0956792507007188 Published online by Cambridge University Press

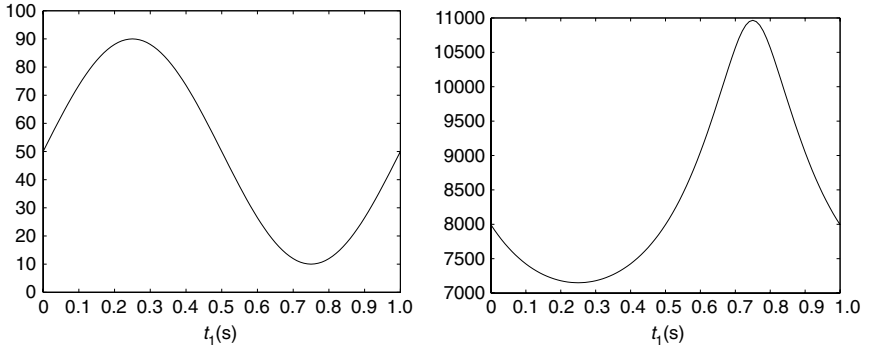

FIGURE 9. Input signal C_3[nF] (left) and resulting local frequency ν[s^{-1}] (right).

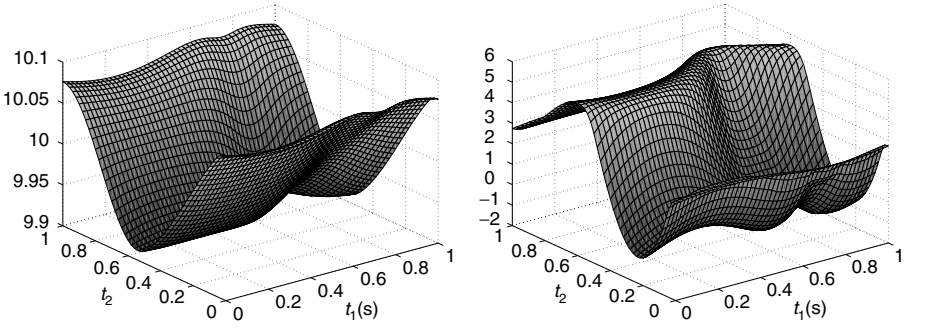

FIGURE 10. MVFs $\hat{U}_1$[V] (left) and $\hat{U}_4$[V] (right).

The time-dependent capacitance (3.41) introduces frequency modulation at widely separated time scales. Thus, we apply the warped MPDE model corresponding to the ODE (3.39). The phase condition (3.20) with $\eta \equiv 0$ is added to determine the local frequency function. To solve the biperiodic boundary value problem (2.11), we use the method of characteristics from Section 3.2.2. We solve the boundary value problem (3.34),(3.35) for ODEs by the shooting method, where trapezoidal rule is applied as a basic solver in numerical integration. More information concerning this simulation can be found in [28].

Figure 9 (right) shows the local frequency function. The capacitance and the frequency are indirectly proportional: In regions of small capacitances, the frequency is high. This behaviour is typical for LC-oscillators. Consequently, from the phase conditions, we are able to determine physically reasonable frequencies. The MVFs for U_1 and U_4 are shown in Figure 10. Each function exhibits just one oscillation in each coordinate direction, and therefore, an efficient representation is possible. Furthermore, we see the performance of the phase condition (3.20) in the first component.

Finally, we also reconstruct the corresponding quasiperiodic solution of (3.39), using the relation (3.9). For comparison, an initial value problem for (3.39) is solved by the trapezoidal rule, where the MPDE solution provides the starting values. Figure 11 demonstrates the resulting signals for the most interesting component U_4. In the first few cycles, we observe a good agreement between both approximations. In later cycles, a phase shift

https://doi.org/10.1017/S0956792507007188 Published online by Cambridge University Press

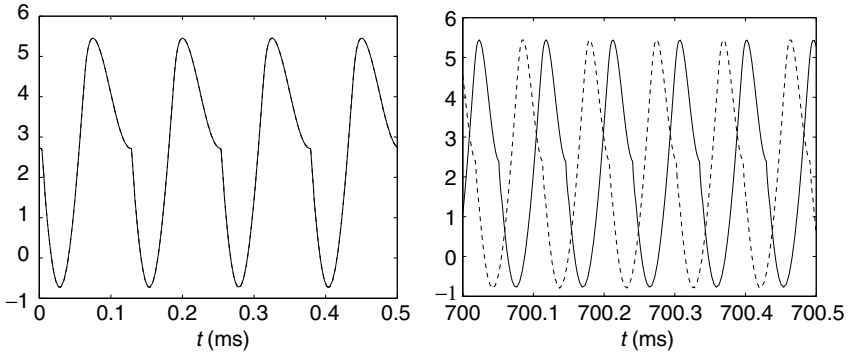

FIGURE 11. ODE solution U_4[V] integrated (solid line) and interpolated from MVFs (dashed line) in time intervals [0 ms, 0.5 ms] (left) and [700 ms, 700.5 ms] (right).

occurs for two reasons. Firstly, small numerical errors in the local frequency function are amplified over many oscillations. Secondly, the transient integration also causes a phase shift in comparison to the exact solution, which represents a more general problem. Nevertheless, the other signal properties agree also in later cycles, i.e., the amplitude, the shape and the frequency.

4 Conclusions and outlook

The simulation of radio frequency circuits is quite time consuming, if based on differential algebraic models commonly used in circuit simulation packages to describe its transient behaviour: here the fast rate restricts the step size in time. This problem can be overcome by replacing multitone signals via multivariate functions and, correspondingly, by transforming the DAE model into a singular PDE model. This transition decouples the widely separated time scales of RF signals and allows for a reconstruction of the original time-dependent signal. The arising modelling approach can be generalised from systems with only amplitude modulation to systems with amplitude and/or frequency modulation. For both MPDAE models, the original and the warped version, different numerical techniques proposed so far in the literature have shown their practicability in numerical simulations of RF circuits.

Two important questions remain to be addressed in the future: on the one hand, it has to be investigated whether modelling via MPDAEs can be applied in an efficient way to other areas of application besides RF circuits. For example, flexible multibody systems might be a promising starting point. On the other hand, adequate strategies for partitioning a circuit by introducing appropriate couplings are desirable, which allow to apply the MPDAE model to several subcircuits separately. In a complex circuit, the individual parts possibly exhibit different multirate behaviour and, therefore, each subcircuit may require its own MPDAE system or an alternative technique in case of completely aperiodic time scales.

https://doi.org/10.1017/S0956792507007188 Published online by Cambridge University Press

Acknowledgements

This work is part of the BMBF programme "Multiskalensysteme in Mikro- und Optoelektronik" within the project "Partielle Differential-Algebraische Multiskalensysteme für die Numerische Simulation von Hochfrequenz-Schaltungen" (No. 03GUNAVN).

References

[1] Brachtendorf, H. G. & Laur, R. (2000) Multi-rate PDE methods for high Q oscillators. In: N. Mastorakis, (editor), *Problems in Modern Applied Mathematics*. CSCC 2000, MCP 2000, MCME 2000 Multi-conference, Athens, July 2000. World Scientific 2000, pp. 391–398.

[2] Brachtendorf, H. G., Welsch, G., Laur, R. & Bunse-Gerstner, A. (1996) Numerical steady state analysis of electronic circuits driven by multi-tone signals. *Electric. Eng.* **79**, 103–112.

[3] Brachtendorf, H. G., Welsch, G. & Laur, R. (1997) A novel time-frequency method for the simulation of the steady state of circuits driven by multi-tone signals. *IEEE Int. Symp. Circuits Syst.* **9**, 1508–1511.

[4] Brachtendorf, H. G., Welsch, G. & Laur, R. (1998) A time-frequency algorithm for the simulation of the initial transient response of oscillators. In: *Proceedings of 1998 IEEE International Symposium on Circuits and Systems*, pp. 296–299.

[5] Chua, L. O. & Ushida, A. (1981) Algorithms for computing almost periodic steady-state response of non-linear systems to multiple input frequencies. *IEEE Trans. CAS 28* **10**, 953–971.

[6] Estèvez Schwarz, D. & Tischendorf, C. (2000) Structural analysis for electric circuits and consequences for modified nodal analysis. *Int. J. Circ. Theor. Appl.* **28**, 131–162.

[7] Günther, M. & Feldmann, U. (1999) CAD based electric circuit modeling in industry I: Mathematical structure and index of network equations. *Surv. Math. Ind.* **8**, 97–129.

[8] Günther, M., Feldmann, U. & ter Maten, E. J. W. (2005) Modeling and discretization of circuit problems. In: W.H.A. Schilders & E. J. W. ter Maten (editors), *Handbook of Numerical Analysis*. Special Volume Numerical Analysis of Electromagnetism. Elsevier North Holland, Amsterdam, 523–659.

[9] Hairer, E., Lubich, C. & Wanner, G. (2006) *Geometric Numerical Integration: Structure-Preserving Algorithms for Ordinary Differential Equations*. Springer, Berlin.

[10] Hairer, E., Nørsett, S. P. & Wanner, G. (1993) *Solving Ordinary Differential Equations. Vol. 1: Nonstiff Problems*. (2nd ed.). Springer, Berlin.

[11] Hairer, E. & Wanner, G. (1996) *Solving Ordinary Differential Equations. Vol. 2: Stiff and Differential-Algebraic Equations*. (2nd ed.). Springer, Berlin.

[12] Ho, C. W., Ruehli, A. E. & Brennan, P. A. (1975) The modified nodal approach to network analysis. *IEEE Trans. CAS* **22**(6), 505–509.

[13] Houben, S. H. M. J. (2004) Simulating multi-tone free-running oscillators with optimal sweep following. In: W. H. A. Schilders, E. J. W. ter Maten & S. H. M. J. Houben (editors), *Scientific Computing in Electrical Engineering*. Mathematics in Industry 4, Springer, Berlin, pp. 240–247.

[14] Horneber, E. H. (1976) *Analyse nichtlinearer RLCÜ-Netzwerke mit Hilfe der gemischten Potentialfunktion mit einer systematischen Darstellung der Analyse nichtlinearer dynamischer Netzwerke*. PhD Thesis, University Kaiserslautern.

[15] Kampowsky, W., Rentrop, P. & Schmitt, W. (1992) Classification and numerical simulation of electric circuits. *Surv. Math. Ind.* **2**, 23–65.

[16] Knorr, S. & Günther, M. (2006) Index analysis of multirate partial differential–algebraic systems in RF-circuits. In: A. M. Anile, G. Alì & G. Mascali (editors), *Scientific Computing in Electrical Engineering*. Mathematics in Industry 9, Springer, Berlin, pp. 93–100.

[17] Knorr, S. & Feldmann, U. (2006) Simulation of pulsed signals in MPDAE-modelled SC-circuits. In: A. Di Bucchianico, R. M. M. Mattheij & M. A. Peletier, (editors), *Progress in Industrial Mathematics at ECMI 2004*. Mathematics in Industry 8, Springer, Berlin, pp. 159–163.

[18] Kundert, K. S., Sangiovanni-Vincentelli, A. & Sugawara, T. (1988) Techniques for finding the periodic steady-state response of circuits. In: T. Ozawa, (editor), *Analog Methods for Computer-Aided Circuit Analysis and Diagnosis*. Marcel Dekker Inc., New York, pp. 169–203.

[19] Lang, B. (2002) *Einbettungsverfahren für Netzwerkgleichungen*. PhD Thesis, University Bremen, Shaker, Aachen.

[20] Lehtovuori, A. (2003) *Multivariate Steady-State Time-Domain Analysis Method*. Master's thesis, Helsinki University of Technology.

[21] Lehtovuori, A., Virtanen, J. & Valtonen, M. (2003) GMRES preconditioner for multivariate steady-state time-domain method. In: *Proceedings of IMS'2003*, Philadelphia, 8–13 June 2003, pp. 2129–2132.

[22] Narayan, O. & Roychowdhury, J. (2003) Analyzing oscillators using multitime PDEs. *IEEE Trans. CAS I*, **50**, 894–903.

[23] Ngoya, E. & Larcheveque, R. (June 1996) Envelop transient analysis: A new method for the transient and steady state analysis of microwave communication circuits and systems. *IEEE Microwave Theory Tech. Symp. Digest*, 1365–1368.

[24] Pulch, R. & Günther, M. (2002) A method of characteristics for solving multirate partial differential equations in radio frequency application. *Appl. Numer. Math.* **42**, 397–409.

[25] Pulch, R. (2003) Finite difference methods for multi time scale differential algebraic equations. *Z. Angew. Math. Mech.* **83**(9), 571–583.

[26] Pulch, R. (2003) A parallel finite difference algorithm for multirate partial differential algebraic equations. In: K. Antreich, R. Bulirsch, A. Gilg & P. Rentrop, (editors), *Modeling, Simulation and Optimization of Integrated Circuits*. International Series of Numerical Mathematics (2004) Vol. 146, Birkhäuser, Basel, pp. 153–166.

[27] Pulch, R. (2004) *PDAE Methoden zur numerischen Simulation quasiperiodischer Grenzzyklen von Oszillatorschaltungen*. PhD Thesis, Munich University of Technology, VDI, Düsseldorf.

[28] Pulch, R. (2005) Multi time scale differential equations for simulating frequency modulated signals. *Appl. Numer. Math. 53*(2–4), 421–436.

[29] Pulch, R. (2006) Warped MPDAE models with continuous phase conditions. In: A. Di Bucchianico, R. M. M. Mattheij & M. A. Peletier (editors), *Progress in Industrial Mathematics at ECMI 2004*. Mathematics in Industry 8, Springer, Berlin, pp. 179–183.

[30] Pulch, R. (2006) Semidiscretisation methods for warped MPDAEs. In: A. M. Anile, G. Alì & G. Mascali (editors), *Scientific Computing in Electrical Engineering*. Mathematics in Industry 9, Springer, Berlin, pp. 101–106.

[31] Pulch, R. (submitted for publication) Variational methods for solving warped multirate partial differential algebraic equations. *SIAM J. Sci. Comput*.

[32] Roychowdhury, J. (1997) Efficient methods for simulating highly non-linear multi-rate circuits. In *Design Automation Conference*, Chiba, Japan, pp. 269–274.

[33] Roychowdhury, J. (2001) Analysing circuits with widely-separated time scales using numerical PDE methods. *IEEE Trans. CAS I 48* **5**, 578–594.

[34] Simeon, B., Arnold, M. (2000) Coupling DAE's and PDE's for simulating the interaction of pantograph and catenary. *Math. Comp. Model. Syst.* **6**, 129–144.

[35] Striebel, M. (2006) *Hierarchical Mixed Multirating for Distributed Integration of DAE Network Equations in Chip Design*. PhD Thesis, University of Wuppertal, VDI, Düsseldorf.

[36] Tischendorf, C. (1999) Topological index calculation of differential–algebraic equations in circuit simulation. *Surv. Math. Ind.* **8**, 187–199.

[37] Ushida, A. & Chua, L. O. (1984) Frequency-domain analysis of non-linear circuits driven by multi-tone signals. *IEEE Trans. CAS 31* **9**, 766–779.

[38] Zhu, L. L. & Christoffersen, C. E. (2005) Fast transient analysis of oscillators using multiple time scales with accurate initial conditions. In: *IEEE Canadian Conference on Computer and Electrical Engineering Digest*, Saskatoon, May 2005, pp. 700–703.

[39] Zhu, L. L. & Christoffersen, C. E. (2005) Adaptive harmonic balance analysis of oscillators using multiple time scales. In: *3rd International IEEE Northeast Workshop on Circuits and Systems Digest*, Quebec, Canada, June 2005, pp. 187–190.